2016

Issues in Laser Induced Breakdown Spectroscopy for Measurements in the Deep Ocean and Other High-Pressure Environments

Joseph C. Bonvallet
University of South Carolina

Issues in Laser Induced Breakdown Spectroscopy for Measurements in the Deep Ocean and other High-Pressure Environments

by

Joseph C. Bonvallet

Bachelor of Science
University of South Carolina, 2010

Submitted in Partial Fulfillment of the Requirements

For the Degree of Doctor of Philosophy in

Chemistry

College of Arts and Sciences

University of South Carolina

2016

Accepted by:

S. Michael Angel, Major Professor

Stephen L. Morgan, Committee Member

Michael L. Myrick, Committee Member

Christopher T. Williams, Committee Member

Lacy Ford, Senior Vice Provost and Dean of Graduate Studies

DEDICATION

I dedicate this work to my wife, Ashleigh, and new baby girl, Rebecca Ann, family, and friends; I could not have made it here today with out your countless words of encouragement and support.

ACKNOWLEDGEMENTS

I would first like to thank my advisor, Dr. S. Michael Angel, his passion for science is contagious, and I appreciate the hours he has spent discussing with me how to solve many different problems. Some of the solutions were as easy as forgetting to turn the power on, others were more difficult.

I would also like to thank my family. Without their insights and support none of this would have been possible. It is because of them that I have survived this journey, particularly the last 4 months. I am forever grateful for my wife that has been an endless well of encouragement.

Lastly, I would like to thank my colleagues in the Angel Group, past and present: Janna Register, Nate Gomer, Nirmal Lamsal, Alicia Strange, Patrick Barnett, Josh Huntington, and Ashley Allan. Many of you I have leaned on significantly along the way. One thing that sets our lab apart from everyone else is the strong feeling of camaraderie and family.

ABSTRACT

This dissertation describes fundamental and applied studies that have advanced the understanding and application laser induced breakdown spectroscopy (LIBS) to the deep-ocean environment and to operation on a deep-ocean submersible. Chapter one is an overview of LIBS including a brief history, LIBS theory, the instrumentation typically used, and a specific application. Chapter two analyzes the effect that monodisperse suspended particles have on LIBS emission intensity and on the formation of a LIBS plasma. This chapter demonstrates that for particle concentrations similar to those found in the neutrally buoyant regions around hydrothermal vents there is little effect on the LIBS emission intensity. Also, this chapter shows that by using 532 nm excitation and a 180˚ collection geometry, strong stimulated Raman of water appears at 649 nm in the spectrum. Chapter three describes an investigation into the use of hydrogen and oxygen as an internal standard for lithium and potassium in bulk aqueous solution. These investigations reveal that the precision in the measured LIBS signal for Li and K is improved by using H or O as an internal standard, with oxygen providing up to a 9-fold improvement in the relative standard deviation (RSD). Finally, chapter four describes the construction and tests of a super critical CO_2 LIBS cell for LIBS measurements of samples in a Venus-type atmosphere.

TABLE OF CONTENTS

LIST OF TABLES

LIST OF FIGURES

CHAPTER 1

REVIEW OF LASER INDUCED BREAKDOWN SPECTROSCOPY

1.1 BACKGROUND ON LIBS

Since first being reported in a meeting abstract by Brech and Cross in 1962 there have been many characteristics that make LIBS an appealing spectroscopic technique for elemental analysis.[1] This relatively simple measurement yields simultaneous sensitivity to many elements in the parts-per-million (ppm) range for solids, liquids, gases and aerosols. LIBS is effectively non-invasive due to the very small sampling region (typically, pg to ng of material are transformed to plasma), no sample preparation required, and LIBS can be used in a standoff mode without perturbing the target. It is also fast, requiring under 1 s for a measurement, and hence is essentially a real-time measurement. These characteristics are some of the greatest advantages of LIBS compared to other analytical approaches.[2, 3] No other sensor is capable of detecting all classes of chemical compounds and all types of matter like LIBS. However, LIBS has never been tested at deep ocean hydrothermal vents.

Figure 1.1 shows a basic experimental setup for high pressure underwater LIBS. A laser pulse having energy of a few tens of mJ and a pulse width of a few ns, can produce a power density larger than the breakdown threshold of most materials (typically, GW/cm^2).[4] This laser ablates and atomizes the sample material. The atoms continue to gain energy from the laser and a high temperature plasma is formed. The

excited atoms in the plasma go from an excited energy level to a lower energy and emit photons. The light is collected and focused onto a fiber optic, which is connected to a spectrometer with a gated intensified charged coupled device (ICCD) detector.[5] The power densities used for LIBS depend on the particular application and the breakdown threshold of the material being analyzed. Breakdown thresholds are typically lower for condensed phases of matter and must be determined for each particular set of conditions.

Radiation from a laser-induced plasma is generally categorized into three types; inverse Bremsstrahlung radiation, recombination radiation, and line emission.[4] The plasma is initiated on the picosecond time scale by weak multiphoton ionization and grows as energy is absorbed for the remainder of the laser pulse through cascade ionization. Ionization is high at the beginning of the plasma, and the emission signal is mostly composed of a broad continuum. This continuum is due to inverse Bremsstrahlung and recombination events. Inverse Bremsstrahlung, or "breaking radiation", is the emission of photons by free electrons that are accelerated or decelerated in collisions.[3,6,7] Recombination radiation is when a free electron goes from a higher ionic or atomic energy level to the ground state and in the process emits a photon. The continuum is a broad spectral emission that overwhelms the atomic line emission that may be present at the beginning of the plasma and acts as a noise source in the LIBS spectra. As the electrons recombine with ions and the plasma cools, line emission becomes more dominant because continuum emission typically decays at a faster rate than line emission. [8] Emission lines provide information about the atomic composition of the sample. The line wavelengths and intensities exhibited by the atoms in the plasma

can be compared to standard libraries of spectral data maintained by NIST. The emission lines can also be calibrated against samples of known makeup.

Since continuum emission from early in the plasma cannot be reduced by averaging, detector gating is used to select a delay time when the continuum has decayed, making line emission clearly visible.[5] The key parameters for time-resolved detection are the gate delay (t_d) and the gate width (t_w). The gate delay is the time between plasma formation and when the ICCD is turned on. The gate width is the ICCD exposure time. These parameters must be optimized for the best signal-to-noise ratio for each element and emission line.[2,9,10] Figure 1.2 shows the timing of a SP-LIBS experiment and how proper gating can reduce the continuum emission. Plasma lifetimes for solids at atmospheric pressure is typically 30-50 μs, but as short at 50-650 ns in liquids and at high pressure because of severe plasma quenching.

1.2 LIBS IN BULK AQUEOUS SOLUTION FOR DEEP OCEAN MEASUREMENTS

Applications of LIBS to aqueous samples have not been as plentiful as for solids. Sampling approaches used for LIBS of liquids include the measurement of aerosols, surface measurements, frozen aqueous solutions, and bulk under water measurements of solutions. LIBS of aerosols is difficult because the individual droplets act as micro-lenses, causing premature laser breakdown.[11,12] This sampling technique has been applied to the detection of heavy metals in drinking water and reported limits of detection (LOD) for cadmium, lead, and zinc have been reported at ~ 0.20 ppm.[11]

Sampling the surface of the solution is a simple approach that has been used by many researchers. This method is similar to sampling the surface of a solid. It is only

suitable for applications where the surface of the solution is a homogeneous representation of the whole solution and is complicated by sample splashing.[13,14]

Sampling frozen solutions can be used as an alternative to liquid solutions in some cases. There are many advantages, such as no sample splashing or reduction of emission intensity due to quenching. However there are several drawbacks such as; practicality, sample handling, and adaptability to remote analysis.[15] This type of sample analysis has been carried out to measure sodium and aluminum in real environmental samples finding a LOD of 1 and 2 ppm, respectively.[15] None of these techniques are applicable to deep ocean underwater LIBS measurements.

Bulk analysis is characterized by focusing the laser pulse under a liquid surface to create the analytical plasma. Bulk solution LIBS is done in two ways, using single pulse (SP) or dual pulse (DP) excitation. LIBS has been investigated for measurements in bulk aqueous solutions since 1969. At that time it was to study the fundamentals of the "explosion" formed in water by a single laser pulse.[16] However, bulk aqueous-phase research on LIBS was on the decline until Cremers et al. demonstrated DP-LIBS in solution for the first time in 1984. This work showed that by using two laser pulses separated in time by a short delay (~50 ns), an increase in detection limit is observed. The first laser pulse forms a gaseous bubble and the second pulse forms a plasma at the liquid gas interface,[17] raising the effective pulse energy.[17-20]. DP-LIBS provides significant emission intensity enhancement in solution over SP-LIBS at atmospheric pressure. DP-LIBS has been studied in high-pressure bulk aqueous solution with emission enhancements at pressures up to ~100 atm at which point the bubble formed by the first laser pulse quickly collapses.[6, 9, 21, 22] This is depicted below in Figure 1.3. Angel *et al.*

also showed that the emission intensity and peak widths for SP-LIBS are unaffected by solution pressure up to ~300 atm.[9, 23]

There are many difficulties associated with LIBS analysis in bulk solution. It has been shown that water quenches the plasma (much of the plasma energy goes into vaporizing the liquid) resulting in a decrease in the emission intensity for most elements.[2, 6, 7] This means the duration of the spectral emission is very short (microseconds) compared to tens of microseconds in air.[7] Compared to solids, the breakdown threshold is also much greater in aqueous solutions. The LIBS emission in solution also exhibits spectral line broadening due to Stark broadening and collisional broadening effects.[6, 24]

1.3 Hydrothermal Vents

Hydrothermal vents are located at mid-ocean ridges on the ocean floor at depths of 800-3600 m. The fluid that exits hydrothermal vents is very hot (~623 K), under extreme pressure (147-361 atm), and is very corrosive.[2, 6, 25] As seawater seeps through the permeable ocean crust, there is an exchange of ions between the fluid and the surrounding rock. As the fluid goes deeper, magma chambers begin to heat the fluid, making it buoyant and it rises back through the crust. Again, ions are exchanged as the temperature changes until the fluid exits the crust through a hydrothermal vent site.[2, 6, 25] This cyclic process is depicted in Figure 1.4.

The physical and chemical dynamics of hydrothermal vents are studied by either collecting samples or using a chemical sensor. Collecting samples and bringing them back to the lab for analysis is not ideal because changes in temperature and pressure affect the chemistry of the samples and only a limited number of samples can be obtained

each time. Few chemical sensors have been developed that can survive the conditions at the vents. One of the few types of chemical sensors that have been used at the vents includes voltammetric sensors. These sensors have been used to detect O_2(aq), Fe(II), and H_2S *in situ*.[26] These compounds have been suggested to control biological communities at hydrothermal vent sites.[26] Voltammetric sensors have slower acquisition times than LIBS.[26]

1.4 Application of LIBS to Hydrothermal Vent Studies

The ongoing long-term goal of this project is to apply LIBS to vent chemistry measurements. Two specific deep-ocean hydrothermal vent experiments drive the laboratory studies. First, determining the spatial and temporal distribution of vent plumes using Li as a tracer. Secondly, measuring the changes in key vent chemical concentrations caused by phase separation events.

Hydrothermal vents expel buoyant plumes of hot water and this water rises to heights of hundreds of meters above the seafloor. The physical and chemical dynamics of the plumes are poorly understood despite their importance in dispersing vent fluids into the oceans.[27] Lithium can be used as a tracer for hydrothermal vent fluids because in seawater it is at a very low concentration (0.18 ppm). However, in vent waters it has been shown to be as high as 9 ppm because it is leached from the host rock in the vent fluid cycle.[28] Monitoring lithium *in situ* would allow oceanographers to track streams of fluid exiting the vents in the ocean.

The elemental concentration of hydrothermal vent fluids can change rapidly between one phase and the other.[29] Under the high temperature and pressure conditions

at hydrothermal vents, a lower-salinity vapor phase may separate and move away from the higher-salinity liquid phase. Each phase contains a distinctly different combination of dissolved materials. Table 1.1 shows elemental concentrations at the 9˚ N area on the East Pacific Rise measured in 1991 and again in 1994.[30] The low concentrations in 1991 correspond to a vapor phase right after an eruption event. In 1994 samples were again taken and correspond to a high salinity liquid phase being released. The limits of detection (LOD) for LIBS are low enough that studying changes in element concentrations following phase separation events at the vents should be possible.

1.4 References

1. Brech, F.; Cross, L., Optical microemission simulated by a ruby maser, Appl. Spectrosc., 1962. 16.

2. Angel, S.M.; Bonvallet, J.; Lawrence-Snyder, M.; Pearman, W.F.; Register, J.; Underwater measurements using laser induced breakdown spectroscopy. J. Anal. At. Spectrom., 2016. 31: 328-336.

3. Scaffidi, J.; Angel, M.S.; Cremers, D., Emission Enhancement Mechanisms in Duel-Pulse LIBS, Anal. Chem. 2006. 41; 25-32.

4. Omenetto, N.; Hahn, D.; Laser-Induced Breakdown Spectroscopy (LIBS), Part I: Review of Basic Diagnostics and Plasma-Particle Interactions: Still-Challenging Issues Within the Analytical Plasma Community, Appl. Spec., 2010. 64; 335A-366A.

5. Cremers, D., Radziemski,L.J.; Handbook of Laser-induced Breakdown Spectroscopy. Chichester, West Sussex, England: John Wiley & Sons, 2006. Print.

6. Michel, A.; Chave, A. Double pulse laser-induced breakdown spectroscopy of bulk aqueous solutions at oceanic pressures: interrelationship of gate delay, pulse energies, interpulse delay, and pressure, Appl. Optics. 2008. 47; G131-G143.

7. De Giacomo, A.; Aglio, M.; Pascale, O. Single Pulse-Laser Induced Breakdown Spectroscopy in aqueous solution, Appl. Phys. A. 2004. 79; 1035-1038.

8. Ingle, James D., and Stanley R. Crouch. Spectrochemical Analysis. Englewood Cliffs, NJ: Prentice Hall, 1988.

9. Lawrence-Snyder, M.; Scaffidi, J.; Angel, S.M.; Michel, A.;Chave, A. Sequential-Pulse Laser –Induced Breakdown Spectroscopy of High-Pressure Bulk Aqueous Solutions, Appl. Spec. 2007. 61; 171-176.

10. Miziolek, Andrzej W., V. Palleschi, and Israel Schechter. Laser-induced Breakdown Spectroscopy (LIBS): Fundamentals and Applications. Cambridge, UK: Cambridge UP, 2006.

11. Essin, M.; Radziemski, L., Sneddon, J., Detection of Cadmium, Lead and Zinc in Aerosols by Laser-Induced breakdown Spectroscopy, J. Anal. At. Spectrom. 1988. 3; 985-988.

12. Kumar, A.; Yueh, F.; Miller, T.; Singh, S., Detection of trace elements in liquids by laser-induced breakdown spectroscopy with a Meinhard nebulizer, Appl. Optics. 2003. 42; 6040-6046.

13. Fichet, P.; Toussiant, A.; Wagner, J., Laser-induced breakdown spectroscopy: A tool for analysis of different types of liquids, Appl. Phys. A. 1999. 69; S591-S592.

14. Fichet, P.; Menut, D.; Brennetot, R.; Vors, E.; Rivoallan, A., Analysis by laser-induced breakdown spectroscopy of complex solids, liquids, and powders with an echelle spectrometer, Appl. Optics. 2003. 42; 6029-6035.

15. Caceres, J.; Lopez, J.; Telle, H.; Urena, A., Quantitative analysis of trace metal ions in ice using laser-induced breakdown spectroscopy, Spectrochim. Acta Part A. 2001. 56; 831-838.

16. Buzukov, A.; Popov, Y.; Teslenko, V., Experimental study of explosin caused by focusing monopulse laser radiation in water, Jour. Appl. Mech. Tech. Phys. 1969. 10; 701-708.

17. Cremmers, D.; Radziemski, L.; Loree, T., Spectrochemical Analysis of Liquids Using the Laser Spark, Appl. Spec. 1984. 38; 721-729.

18. De Giacomo, A.; Dell'Aglio, M.; De Pascale, O.; Capitelli, M., From single pulse to double pulse ns-Laser Induced Breakdown Spectroscopy under water: Elemental analysis of aqueous solutions and submerged solid samples, Spectrochim. Acta Part B. 2007. 62; 721-738.

19. Casavola, A., De Giacomo, A., Dell'Aglio, M., Taccogna, F., Colonna, G., De Pascale, O., Longo,S., Experimental investigation and modelling of double-pulse laser induced plasma spectroscopy under water, Spectrochim. Acta, 2005. 60; 975-985.

20. Lazic, V., S. Jovicevic, R. Fantoni and F. Calao, Efficient plasma and bubble generation underwater by an optimized laser excitation and its application for liquid

analyses by laser-induced breakdown spectroscopy, Spectrochimica Acta Part B, 2007. 62; 1433-1442.

21. Gaudiuso, R., M. Dell'Aglio, O. De Pascale, G.S. Senesi & A. De Giacomo. Laser induced breakdown spectroscopy for elemental analysis in environmental, cultural heritage and space applications: A review of methods and results, Sensors, 2010. 10; 7434-7468.

22. Takahashi, T., Thornton, B., Sato, T., Ohki, K., & Sakka, T. Quantitative chemical analysis of submerged solids using calibration-free laser-induced breakdown spectroscopy. Proc. MTS/IEEE Oceans '14, St. John's, NL, 2014. 140326-120.

23. Ahmed, R.; Baig, A., A comparative study of single and double pulse laser induced breakdown spectroscopy, J. Appl. Phys. 2009. 106; 033307-1-033307-6.

24. Tognoni, E.; Palleschi, V.; Corsi, M.; Cristoforetti, G., Quantitative micro-analysis by laser-induced breakdown spectroscopy: a review of the experimental approaches, Spectrochim. Acta Part A. 2002. 57; 1115-1130.

25. Michel, A.; Lawrence-Snyder, M.; Angel, S.M.; Chave, A., Laser-induced breakdown spectroscopy of bulk aqueous solutions at oceanic pressures: evaluation of key measurement parameters, Appl. Optics. 2007. 46; 2507-2515.

26. Luther, G.; Rozan, T.; Taillefert, M.; Nuzzio, D.: Meo, C.; Shank, T.; Lutz, R.; Cary, S., Chemical speciation drives hydrothermal vent ecology, Nature. 2001. 410; 813-816.

27. Elderfield, H.; Schultz, A., Mid-Ocean ridge hydrothermal fluxes and the chemical composition of the ocean, Annu. Rev. Earth Planet. Sci. 1996. 24; 191-200.

28. Von Damm, K.; Edmond, J.; Grant, B.; Measures, C., Chemistry of submarine hydrothermal solutions at 21˚N, East Pacific Rise, Geochem. Et. Cosmochem. Acta. 1985. 49; 2197-2220.

29. Tivey, M., Generation of Seafloor Hydrothermal Vent Fluids and Assocated Mineral Deposits, Oceanography. 2007. 20; 50-63.

30. Butterfield, D.; Massoth, G., Geochemistry of north Cleft segment vent fluids: Temporal changes in chlorinity and their possible relation to recent volcanism, J. Geophys. Res. 1994. 99; 4951.

Table 1.1. Element concentrations in ppm for the EPR at 9˚ N in 1991 and 1994 [20]

Element	1991 Concentration (ppm)	1994 Concentration (ppm)
Na	883	15709
K	47	1623
Ca	72	1828
Mn	11	181

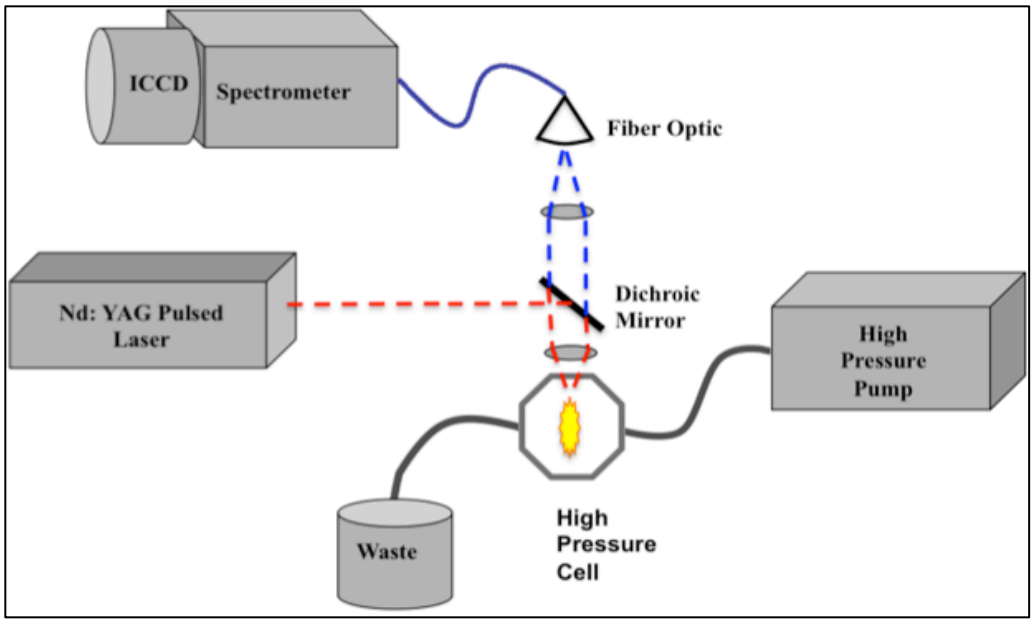

Figure 1.1. Single-pulse LIBS high-pressure setup

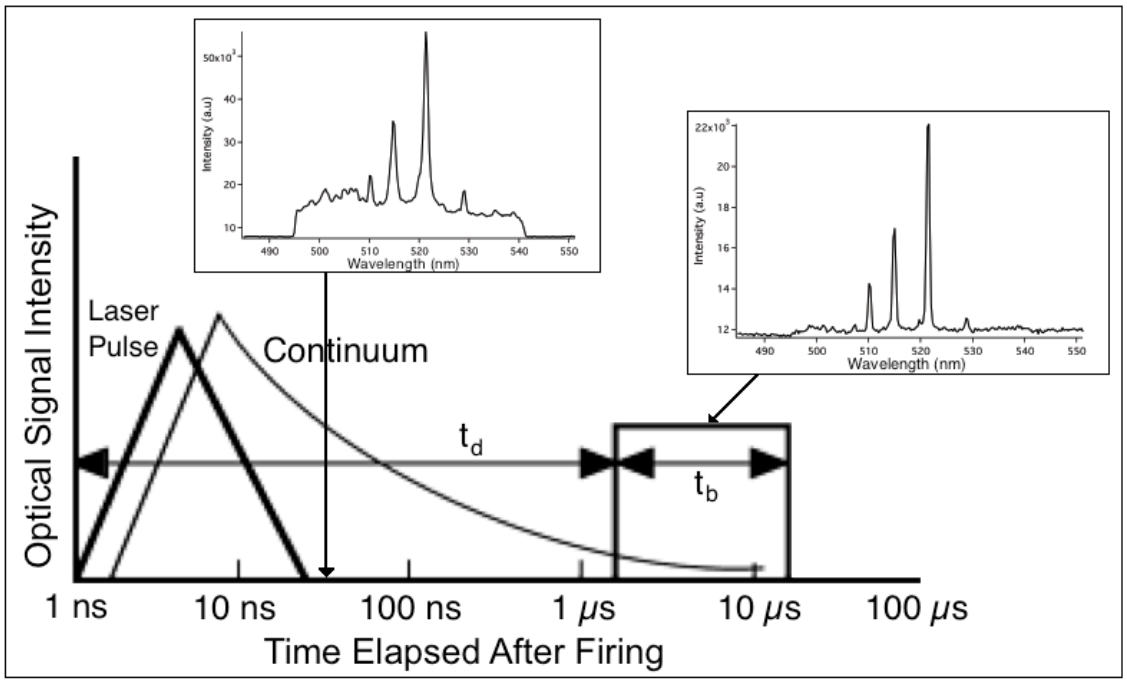

Figure 1.2. Important timing periods in a LIBS measurement; gate delay (t_d) and gate width (t_w).[10]

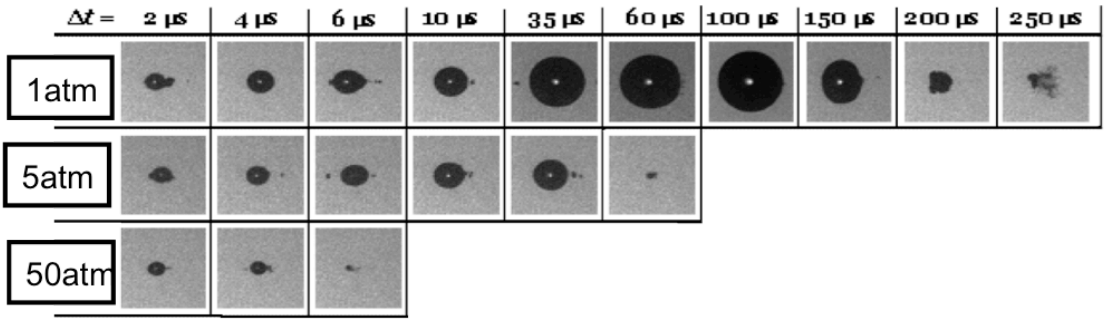

Figure 1.3. The size and lifetime of the LIBS bubble decreases, as the surrounding pressure is increased.[1]

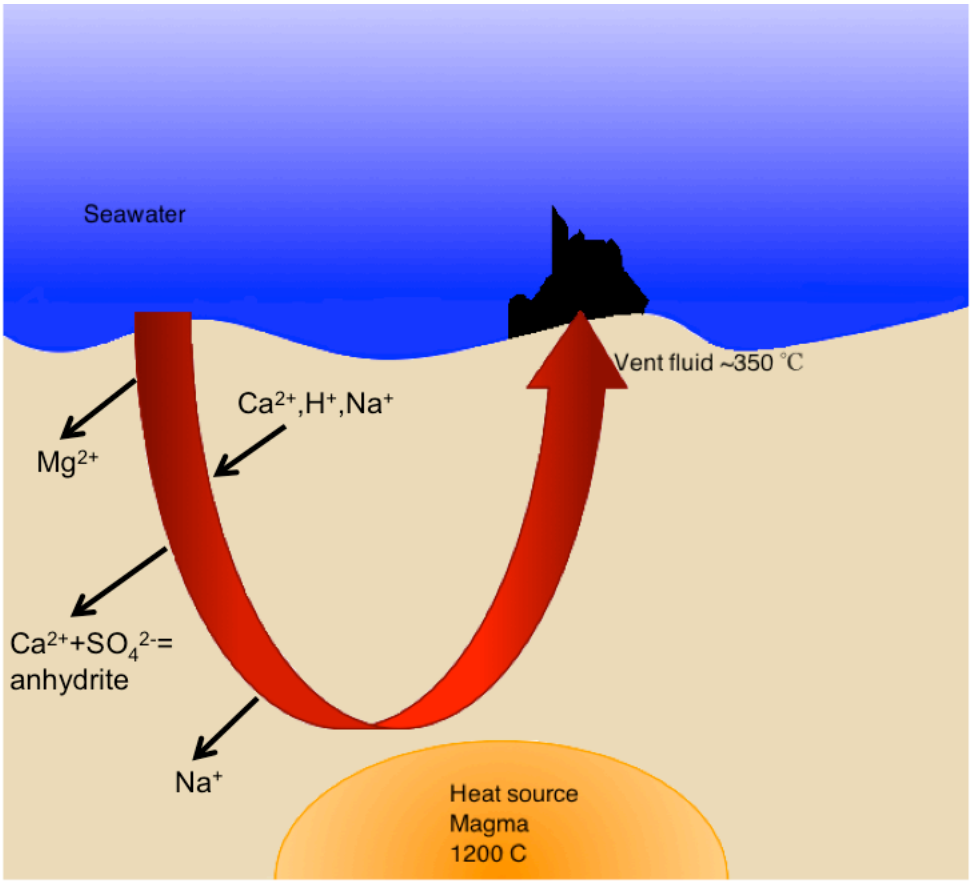

Figure 1.4. Hydrothermal vent fluid cycle.

CHAPTER 2

THE EFFECT OF SUSPENDED PARTICLES ON UNDERWATER LASER INDUCED BREAKDOWN SPECTROSCOPY FOR MEASUREMENTS OF DISSOLVED SPECIES

2.1 ABSTRACT

In this work, the effect of suspended particles on underwater laser induced breakdown spectroscopy (LIBS) of dissolved species in water is being investigated. The emission intensity for dissolved elements decreases linearly with the scattering coefficient of the solution, but the slope is different for different particle sizes. There is little to no effect, on the LIBS emission intensity, for the range of suspended particles (0.8 μm, 2 μm, 6 μm, 12 μm) at concentrations corresponding to the region of neutrally buoyant fluids around hydrothermal vents. For the size and concentration of suspended particles seen at hydrothermal vents the LIBS emission intensity no more than ~10%.

2.2 INTRODUCTION

Since being first reported by Brech and Cross in 1962,[1] laser-induced breakdown spectroscopy (LIBS), has become a widely used analytical method. It is a relatively simple technique that allows for rapid multi-elemental analysis of solids, liquids, and gases with little or no sample preparation. LIBS is also effectively nondestructive, only ablating picogram to nanogram amounts of material with each laser pulse. LIBS is well suited for *in situ* and remote elemental analysis,[2-20] and is particularly useful for

applications in extreme, hostile, and inaccessible environments.[10-18, 21-34] Our interest lies in using LIBS for multi-elemental analysis of high-pressure aqueous solutions, which can be found in the deep ocean at hydrothermal vent sites. [31-34]

Hydrothermal vents are thought to control much of the oceans chemistry.[38] These vent sites occur at mid-ocean ridges on the ocean floor at depths of 800 - 3600 m and pressures of 147-361 atm and expel fluid at extremely high temperatures (200-405 °C).[35] Water seeps through the semi-permeable ocean crust where there is an exchange of ions between the fluid and the surrounding rocks. This ion rich fluid is eventually expelled at one of the vent sites where many of the dissolved species precipitate out to form vent chimneys. Due to the extreme pressure at these depths and the irreversible changes samples undergo when brought back to the surface, and the corrosive nature of the vent fluids, analytical measurements in these environments are difficult.

Despite the high potential of applying LIBS to underwater measurements, there are limited reports on this subject due to the many difficulties. The work of Cremers et al. has showed that LIBS can be used to detect Li, K, Na, Ca, B, Al, Cs, Be, and Rb in bulk aqueous solutions, typically on the part-per-million (ppm) level.[30] The emission intensity under water is greatly reduced, compared to ambient air, due to quenching by the liquid.[16,30,31,33] Additionally, plasma emission lines are usually very short lived, on the order of 1 μs or less compared to ambient air in which typical lifetimes are 5 – 20 μs.

Around hydrothermal vents, lithium can be in the 10s of ppm due to it being leached out of rocks in the Earth's crust by hot vent fluids.[35] Lithium is normally found in the ocean at trace levels, below 1 ppm,[35] which makes it a useful tracer of vent fluids and is useful to map their extent. Large changes in lithium, potassium and several other

element concentrations at vent sites have been shown to be associated with phase separation events with concentrations over 2000 ppm reported.[35-37] Precipitates crash out of vent fluids very quick once they come into contact with the cold deep ocean water (2 C°). These precipitates are what give the vents the appearance that smoke is being expelled, and hydrothermal vents are often referred to as "black smokers". This can cause the surrounding area to have increased levels of particulates, which could scatter both the laser light and the LIBS emission.

Suspended particles can be an issue in LIBS, where particle scatter can reduce both the laser and emission intensity, or interfere with formation of a strong plasma. Baker et al. measured the amount and size of suspended particles extending out from plumes over hydrothermal vent at Juan de Fuca Ridge and found that above and outside the plume boundaries the particle size was ~3 µm with a volume concentration of < 20 ppb. Particles in the neutrally buoyant zone around vent plumes range from .56 µm to 10 µm with a mean particle concentration of 100 ppb.[36-37] The effect of particle scattering on LIBS emission has not be reported. Studies have been carried using monodisperse latex spheres (0.8 µm, 2µm, 6µm, 12µm) suspended in lithium and potassium solutions to see the effect particles have on the LIBS emission.

2.3 EXPERIMENTAL

The experimental setup used in these studies, shown in Figure 2.1, has been previously described in earlier work.[30] All measurements were made at ambient pressure using a Continuum Surelite III Nd:YAG laser for excitation operated at both 1064 nm and 532 nm with a repetition rate of 1 Hz. A laser power of ~115 mJ/pulse for 1064 nm

and ~70 mJ/pulse for 532 nm was typically used for these underwater LIBS measurements. The laser was directed into a custom stainless steel cell with 25.4 mm quartz windows, by reflection from a 45° dichroic mirror (M) and focused ~15 mm into the solution using a 25.4 mm diameter, f/2 fused silica lens. Analyte emission was collected back through the same lens and focused using a second 25.4 mm diameter f/2 lens on to a 2 mm core diameter optical fiber, which was coupled to a f/4 dispersive spectrometer (Chromex Model 250IS/RF) with 300 gr/mm grating blazed at 1 μm, which allowed for a ~200 nm spectral window with about 2.5 nm spectral resolution. The collection system consisted of a gated 1064x256 pixel ICCD (Princeton Instruments I-Max 1024-E).

Test solutions were made by dissolving LiCl (Sigma-Aldrich 255572) in deionized water. To each solution, 1 μL/mL of Triton X-100, a surfactant, was added in order to keep the standardized monodisperse polystyrene latex particles, 0.8 μm, 2 μm, 6 μm, 12 μm (Sigma-Aldrich LB8, 80177, 89756, 88511), suspended. An aliquot of the particles was added to 100 mL of the analyte solution. The scattering coefficient was calculated by measuring the laser transmission of the analyte solution in a 30.1 mm path length cell and subtracting a blank, which contained the same solutions without added particles. The lithium 670 nm and potassium 766 nm emission lines were used for all studies shown.

2.4 Results and Discussion

The presence of particles can effect LIBS emission by attenuation at the laser wavelength and at the atomic emission wavelength by absorption and scattering. Particles

can also change the nature of plasma formation because the breakdown threshold for LIBS on solid particles is lower than water.[40] Attenuation of LIBS emission by particle absorption or scattering is a logarithmic type relationship as shown in Eqn. 1, where m is the combined absorption and scattering loss (i.e., a loss coefficient) at the emission wavelength (m_e) caused by particles in solution and L is the optical pathlength. Attenuation of the laser by particle absorption or scattering leads to two effects. A simple light attenuation effect that follows the same form as Eqn. 2.1, and a more complex effect due to the nonlinear nature of LIBS plasma formation. Over certain ranges of laser power, it has been shown, LIBS emission intensity is linearly proportional to laser power. For this case, an attenuation of emission intensity caused by particle absorption and scattering at the laser wavelength (m_L) would also follow Eqn. 2.1. The total attenuation, T_T, of the emission signal from both effects is shown by Eqn. 2.2.

$$T_e = e^{-mL} \qquad \text{Eqn. 2.1}$$

$$T_T = T_e T_L = e^{-m_e L_L} \qquad \text{Eqn. 2.2}$$

If the optical pathlength is the same for the laser and emission, Eqn. 2 can be written as shown in Eqn. 2.3. If there are no particle affects other than simple attenuation of the laser and LIBS emission, a plot of $\ln(I_{em}/L)$, where I_{em} is the measured LIBS emission, versus the loss coefficient at the laser wavelength should be linear with an intercept equal to the loss coefficient at the emission wavelength. Attenuation at the laser wavelength is done by measuring the laser transmittance through the measurement cell. Attenuation at the emission wavelength is complicated by the LIBS plasma.

$$-\ln(T_T/L) = m_L + m_e \qquad \text{Eqn. 2.3}$$

Figure 2.2 shows the effect of increasing the number of particles of various sizes in solution on the 1064 nm excited LIBS emission of the 670 nm lithium line for 500 ppm Li (Figure 2.2a) and 12.5 ppm Li (Figure 2.2b). In Figure 2.2, the Li emission is plotted as the $\ln(I_p/I_{bl})$, versus number of particles per mL of solution, where I_p is emission intensity with added particles and I_{bl} is emission intensity for a blank sample (i.e., no added particles). Plotted in this way the Li emission drops linearly with particle concentration over a concentration range of several orders of magnitude. The latex particles used are transparent, so the biggest optical effect is attenuation of the laser and LIBS emission by scattering. The 0.8 μm particles are smaller than the laser wavelength, but longer than the 670 nm Li emission wavelength. Thus, both Rayleigh and Mie scattering might be significant for the smaller particles while Mie should dominate for the larger particles. Rayleigh scales as the 3rd power of particle diameter while Mie scattering scales as diameter squared. The data in Figure 2.2 shows a linear relationship of emission with number of scattering particles over a wide range of concentrations. As expected larger particles show a much larger attenuation of the LIBS emission at lower concentrations of particles, consistent with Rayleigh or Mie scattering.

Looking more closely at the magnitude of this effect, Figure 2.2a shows a 19-fold reduction in the LIBS emission intensity for 2 μm versus 0.8 μm particles. This is a little larger than the16-fold reduction in intensity that would be expected if Rayleigh scattering were dominant (i.e., Mie scattering would be much smaller) and the difference might suggest other sources of light emission attenuation. In Figure 2.2a, for particles significantly larger than the wavelength of light (6 μm and 12 μm) a 4-fold difference in emission attenuation is expected from Mie scattering and that is what is observed. The

same basic trends are observed in Figure 2.2b for 12.5 ppm Li, with a 13-fold emission attenuation difference between the 0.8 and 2 µm particles and a 5-fold difference for the 6 µm and 12 µm particles. However, there is a significant vertical offset in the plot for 2 µm particles, suggesting a second source of emission attenuation that is dependent on the Li concentration.

Similar to Figure 2.2, Figure 2.3 shows the effect of increasing the number of particles in solution on the 532 nm excited 670 nm lithium LIBS emission for 500 ppm Li (Figure 2.3a) and 12.5 ppm Li (Figure 2.3b), plotted as $\ln(I_p/I_{bl})$, versus number of particles per mL of solution. In Figure 2.4a, the point marked by a circled cross shows the Li emission attenuation for 0.8 µm particles at 20 ppb (1.07×10^5 particles/mL), the concentration reported by Baker et al for the most abundant size particles (i.e., 2 µm) found in the neutrally buoyant region of the Juan de Fuca hydrothermal vent.[36] As indicated, only a slight reduction, ~5-10%, in the 670 nm Li emission was observed. The 2, 6 and 12 µm particles at ~20 ppb gave similar results.

In Figure 2.3, all the measured particles were significantly larger than the 532 nm laser wavelength, thus mostly Mie type scattering is expected. This is consistent with the slopes of the lines being closer together than the 1064 nm excited data shown in Figure 2.2. Using 1064 nm excitation, the slope of the 0.8 µm particle line is much less than using 532 nm excitation. Mie scattering should lead to a 6-fold difference in LIBS emission attenuation for the 0.8 µm and 2 µm particles, but only a 3-4-fold decrease is observed in Figure 2.3a. A 9-fold difference is expected for the 2 µm and 6 µm particles, but only a ~3-fold difference was measured. Clearly, scattering doesn't completely explain the slope differences.

In Figure 2.3b (12.5 ppm Li) the slope differences are similar to Figure 2.3a, ~4 fold difference for the 0.8 µm and 2 µm particles, and ~2-3 fold for the 6 µm and 12 µm particles. However, at the lower Li concentration the attenuation of the Li emission is much larger for the two smaller particle sizes.

These measurements were also made for potassium solutions and the same trend is seen. Again, Mie scattering should lead to a 6-fold difference in the potassium LIBS emission, however, only a ~3-fold difference was measured for 0.8 µm and 2 µm particles. This indicates that more than just simple light scattering is effecting the potassium emission.

Figure 2.4 shows the Li emission, plotted as $\ln(I_p/I_{bl})$, versus scattering coefficient for 0.8, 2, 6 and 12 µm size particles using 532 nm excitation, for 500 ppm (Figure 2.4a) and 12.5 ppm (Figure 2.4b) Li. The scattering coefficient is directly related to the total number of particles. For a given particle concentration the scattering coefficient scales roughly as the square of the particle diameter. For 500 ppm Li (Figure 2.4a) the y intercept is zero, but the slopes increases as the particles get smaller, indicating decreased Li emission for the smaller particles, for a constant scattering coefficient at the laser wavelength. There is essentially no change in Li emission for the 12 µm particles and the slope is only about -0.35. The reason for this is clear by examining the plasma images shown in Figure 2.5. The images were measured for solutions of all four particle sizes with a scattering coefficient of ~0.25 and lithium concentration of 500 ppm. As particle size increases the plasma become ~2 times more elongated and there are more unique points of breakdown, reducing the optical path length from 3.01 cm to 2.02 cm in the solution. The images also suggest that the slope differences for different size particles is a

combination of changing optical path as well as changes in scattering losses at the Li 670 nm emission wavelength. In Figure 2.4b there is clear separation between the smaller 0.8 and 2 μm particles and the larger 6 and 12 μm particles and there is a significant y-intercept for the smaller particles. This suggests a second source of emission attenuation that is dependent on the Li concentration. The reason for this effect has not yet been investigated.

For LIBS measurements using 532 nm excitation, with 180˚ collection, a strong band at 649 nm appears, seen in Figure 2.6. The 649 nm band has been reported as stimulated Raman for the OH-stretch band of water.[39] Simulated Raman emission from a LIBS plasma is highly directional and propagates counter to the direction of the incident laser beam.[39] In Figure 2.4b, the dotted lines (right axis) show the $\ln(I_{OH,P}/I_{OH,bl})$ of the 649 nm simulated Raman signal versus scattering coefficient for each particle size. Where $I_{OH,P}$ is the OH-stretch intensity with particles added and $I_{OH,bl}$ is OH-stretch intensity without any particles added to the solution. The SR signal is independent of particle size and the intensity decreases quicker than the lithium LIBS emission. This is consistent with generation of the SR signal early in plasma formation before plasma growth. This also suggests that the differences in emission attenuation between the 500 ppm and 12.5 ppm solutions, results from changes in position and intensity of the LIBS plasma.

2.5 Conclusions

For particles of the size and concentration found in the neutrally buoyant part of hydrothermal vent plumes, there is little effect on the intensity of LIBS emission (at most

a ~10% reduction). This work was also extended to particle concentrations several orders of magnitude higher to simulate conditions closer to a vent site. The LIBS emission was linear with increased particles, however the deviation of emission attenuation suggests that another mechanism to be taking place. This could be described by the differences in plasma formation as particle sizes increase and is also a function if the analyte concentration.

2.6 REFERENCES

1. Brech, F.; Cross, L., Optical microemission simulated by a ruby maser, Appl. Spectrosc., 1962. 16; 58.

2. Majidi V.; Joseph, M.; Spectroscopic applications of laser induced plasmas, Crit. Rev. Anal. Chem. 1992. 23; 143–162.

3. Radziemski, L.; Review of analytical applications of laser plasmas and laser ablation, 1987–1994, Microchem. J. 1994. 50; 218–234.

4. Rusak, D.; Castle, B.; Smith, B.; Winefordner, J.; Fundamentals and applications of laser-induced breakdown spectroscopy, Crit. Rev. Anal. Chem., 1997. 27; 257–290.

5. Song, K.; Lee, Y.; Sneddon, J.; Applications of laser-induced breakdown spectrometry, Appl. Spectrosc. Rev. 1997. 32; 183–235.

6. Sneddon, J.; Lee, Y.; Novel and recent applications of elemental determination by laser-induced breakdown spectroscopy, Anal. Lett. 1999. 32; 2143–2162.

7. Rusak, D.; Castle, B.; Smith, B.; Winefordner, J.; Recent trends and the future of laser-induced plasma spectroscopy, Trend. Analyt. Chem. 1998. 17; 453–461.

8. Lee W.; Wu J.; Lee Y.; Sneddon J.; Recent applications of laser-induced breakdown spectrometry: a review of material approaches, Appl. Spectrosc. Rev., 2004. 39; 27–97.

9. Salle, B.; Lacour, J.L.; Vors, E.; Fichet, P.; Maurice, S.; Cremers, D. A.; Wiens R. C., Laser-induced breakdown spectroscopy for Mars surface analysis: capabilities at stand-off distances and detection of chlorine and sulfur elements, Spectrochim. Acta Part B, 2004. 59: 1413–1422.

10. Arp, Z.; Cremers, D.; Harris, R. D.; Oschwald, D.; Parker, G.R. Jr.; Wayne, D.; Feasibility of generating a useful laser induced breakdown spectroscopy plasma on rocks at high pressure: preliminary study for a Venus mission, Spectrochim. Acta Part B 2004. 59; 987–999.

11. Seyfried, W. Jr.; Johnson, K.; Tivey, M. C.; In-situ sensors: their development and application for the study of chemical, physical and biological systems at mid-ocean ridges, NSF_Ridge Sponsored Workshop Report (2000).

12. The next generation of in situ biological and chemical sensors in the ocean: a workshop report, (2004). URL:http://www.whoi.edu/institutes/OLI/activities/symposia_sensors.htm.

13. Daly, K.; Byrne, R.; Dickson, A.; Gallager, S.; Perry, M.; Tivey, M.; Chemical and biological sensors for time-series research: current status and new directions, Mar. Technol. Soc. J., 2004. 38; 121–143.

14. Dickey, T.; The role of new technology in advancing ocean biogeochemical studies, Oceanography 2001. 14; 108–120.

15. Varney, M.; ed., Chemical Sensors in Oceanography (Gordon and Breach, 2000).

16. Pichahchy, A.; Cremers, D.; Ferris, M.; Elemental analysis of metals under water using laser-induced breakdown spectroscopy, Spectrochim. Acta Part B, 1997. 52; 25–39.

17. Fichet, P.; Menut, D.; Brennetot, R.; Vors, E.; Rivoallan, A., Analysis by laser-induced breakdown spectroscopy of complex solids, liquids, and powders with an echelle spectrometer, Appl. Optics. 2003. 42; 6029-6035.

18. Fichet, P.; Mauchien, P.; Wagner, J.F.; Moulin, C.; Quantitative elemental determination in water and oil by laser induced breakdown spectroscopy, Anal. Chim. Acta 2001. 429; 269–278.

19. Arca, G.; Ciucci, A.; Palleschi, V.; Rastelli, S.; Tognoni, E.; Trace element analysis in water by the laser-induced breakdown spectroscopy technique, Appl. Spectrosc. 1997. 51; 1102–1105.

20. Samek, O.; Beddows, D.; Kaiser, J.; Kukhlevsky, S.; Liska, M.; Telle, H. H.; Young, J.; Application of laser-induced breakdown spectroscopy to in situ analysis of liquid samples, Opt. Eng. 2002. 39; 2248-2262.

21. Paksy, L.; Német, B.; Lengyel, A.; Kozma, L.; Czekkel, J.; Production control of metal alloys by laser spectroscopy of the molten metals. Part 1. Preliminary investigations, Spectrochim. Acta Part B, 1996. 51; 279-290.

22. Tran, M.; Sun, Q.; Smith, B.; Winefordner, J.D.; Direct determination of trace elements in terephthalic acid by laser induced breakdown spectroscopy, Anal. Chim. Acta, 2000. 419; 153-158.

23. Wainner, R.T.; Harmon, R.S.; Miziolek, A.W.; McNesby, K.L.; French, P.D.; Analysis of environmental lead contamination: comparison of LIBS field and laboratory instruments, Spectrochim. Acta Part B, 2001. 56; 777-793.

24. Barbini, R.; Colao, F.; Lazic, V.; Fantoni, R.; Palucci, A.; Angelone, M.; On board LIBS analysis of marine sediments collected during the XVI Italian campaign in Antarctica, Spectrochim. Acta Part B, 2002. 57; 1203-1218.

25. Bulajic, D.; Cristoforetti, G.; Corsi, M.; Hidalgo, M.; Legnaioli, S.; Palleschi, V.; Salvetti, A.; Tognoni, E.; Green, S.; Bates, D.; Steiger, A.; Fonseca, J.; Martins, J.; McKay, J.; Tozer, B.; Wells, D.; Wells, R.; Harith, M.A.; Diagnostics of high-temperature steel pipes in industrial environment by laser-induced breakdown spectroscopy technique: the LIBSGRAIN project, Spectrochim. Acta Part B 2002. 57; 1181-1192.

26. Noda, M.; Deguchi, Y.; Iwasaki, S.; Yoshikawa, N.; Detection of carbon content in a high-temperature and high- pressure environment using laser-induced breakdown spectroscopy, Spectrochim. Acta Part B 2002. 57; 701-709.

27. Lee W.; Wu J.; Lee Y.; Sneddon J.; Recent applications of laser-induced breakdown spectrometry: a review of material approaches, Appl. Spectrosc. Rev., 2004. 39; 27–97.

28. Munson, C.A.; De Lucia F.C. Jr.; Piehler, T.; McNesby, K.L.; Miziolek, A.W.; Investigation of statistics strategies for improving the discriminating power of laser-induced breakdown spectroscopy for chemical and biological warfare agent simulates, Spectrochim. Acta Part B, 2005. 60; 1217-1224.

29. Sallé, B.; Cremers, D.A.; Maurice, S.; Wiens, R.C.; Laser-induced breakdown spectroscopy for space exploration applications: Influence of the ambient pressure on the calibration curves prepared from soil and clay samples, Spectrochim. Acta Part B 2005. 60: 479-490.

30. Radziemski, L.; Cremers, D.A.; Benelli, K.; Khoo, C.; Harris, R.D.; Use of the vacuum ultraviolet spectral region for laser-induced breakdown spectroscopy-based Martian geology and exploration, Spectrochim. Acta Part B 2005. 60; 237-248.

31. Lawrence-Snyder, M.; Scaffidi, J.; Angel, S. M.; Michel, A.P.M.; Chave, A.D.; Laser-Induced Breakdown Spectroscopy of High-Pressure Bulk Aqueous Solutions, Appl. Spectrosc. 2006. 60; 786-790.

32. Lawrence-Snyder, M.; Scaffidi, J.; Angel, S.M.; Michel, A.;Chave, A. Sequential-Pulse Laser –Induced Breakdown Spectroscopy of High-Pressure Bulk Aqueous Solutions, Appl. Spec., 2007. 61; 171-176.

33. Michel, A.; Lawrence-Snyder, M.; Angel, S.M.; Chave, A., Laser-induced breakdown spectroscopy of bulk aqueous solutions at oceanic pressures: evaluation of key measurement parameters, Appl. Optics. 2007. 46; 2507-2515.

34. Angel, S.M.; Bonvallet, J.; Lawrence-Snyder, M.; Pearman, W.F.; Register, J.; Underwater measurements using laser induced breakdown spectroscopy. J. Anal. At. Spectrom., 2016. 31; 328-336.

35. Seyfried, W.E., Jr.; Janecky D.R.; Mottl, M.J.; Alteration of the oceanic crust: Implications for geochemical cycles of lithium and boron, Geochimica Acta, 1984. 48; 557-569.

36. Walker, S.L.; Baker, E.T.; Particle-Size Distributions within Hydrothermal Plums Over the Juan de Fuca Ridge, Mar. Geol. 1988. 78; 217-226.

37. Baker, E.T.; Tennant, D.A.; Feely, R.A.; Lebon, G.T.; Walker, S.L.; Field and laboratory studies on the effect of particle size and composition of optical backscattering measurements in hydrothermal vent plumes, Deep-Sea Research I, 2001. 48; 593-604.

38. German, C.R.; Von Damm, K.L.; Hydrothermal processes Treatise on Geochemistry, H. Elderfield, H. D. Holland, and K. K. Turekian, eds. Elsevier. 2003. 6; 181-222.

39. Yui, H.; Kanoh, K.; Fujiwara, H.; Sawada, T.; Stimulated Raman scattering of liquid water under the strong focusing condition: analysis of local hydration network environments in dilute ethanol solutions, J. Phys. Chem. 2002. 106; 12041-12044.

40. Kuvalchuk-Kogan, T.; Butatov, V.; Schechter, I.; Optical Breakdown in Liquid Suspensions and its Analytical Applications, Adv. Chem., 2015. 2015; 1-21.

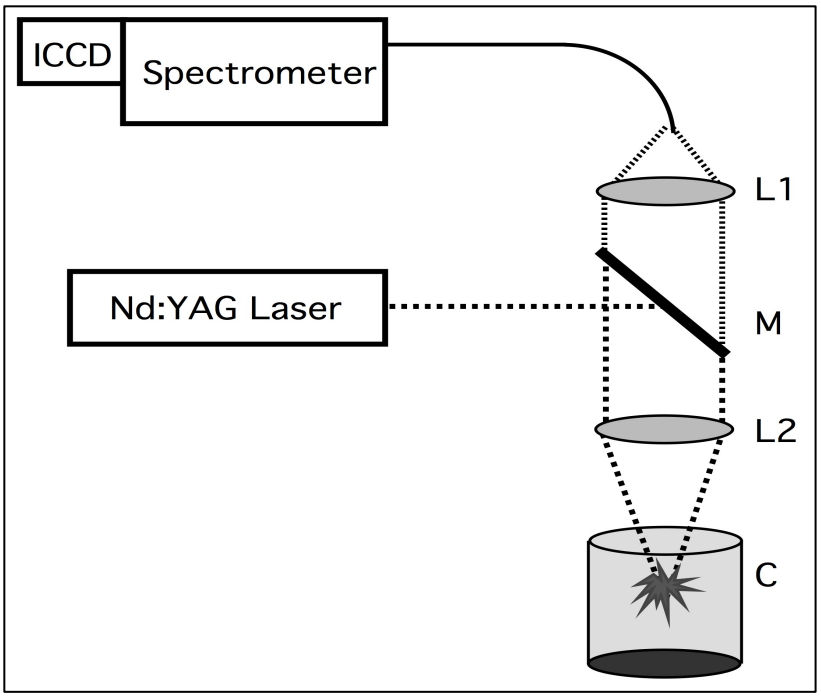

Figure 2.1 Experimental laser induced breakdown spectroscopy set-up. L1 & L2 are f/2 convex lenses, M is a dichroic mirror, C is the sample cell.

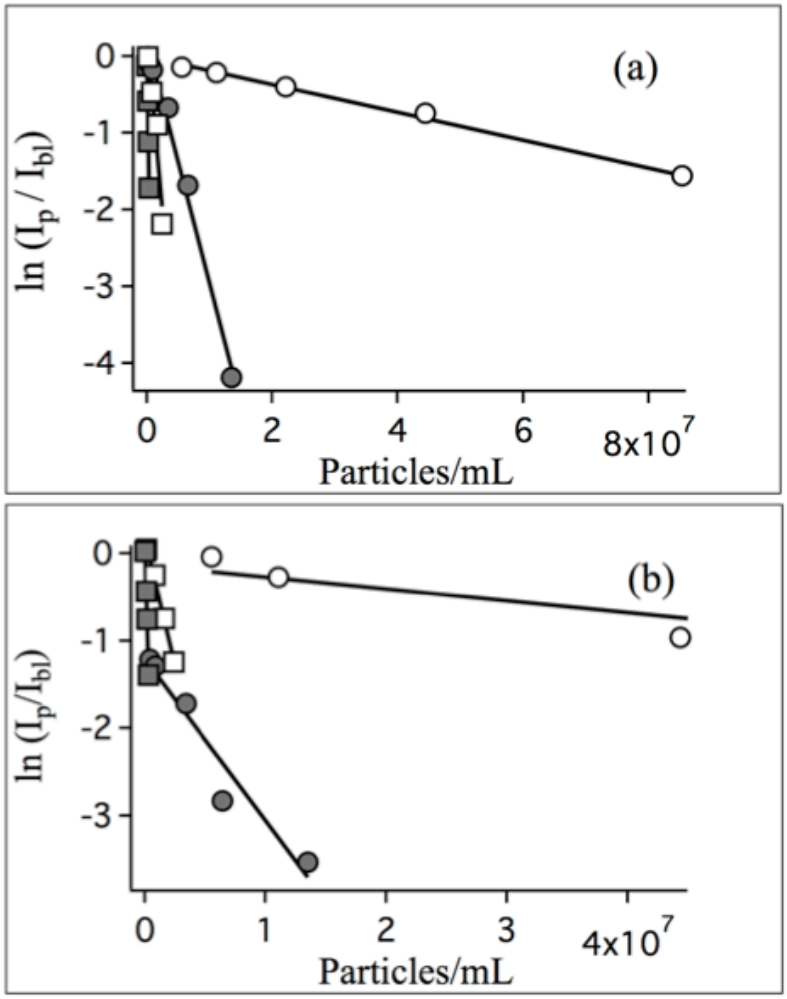

Figure 2.2. Normalized Li intensity verses the total number of latex particles added to the solution using 1064 nm excitation containing monodisperse polystyrene latex particles, 0.8 m (○), 2 µm (●), 6 µm (□), 12 µm (■); (a) 500 ppm Li solution (b) 12.5ppm Li solution.

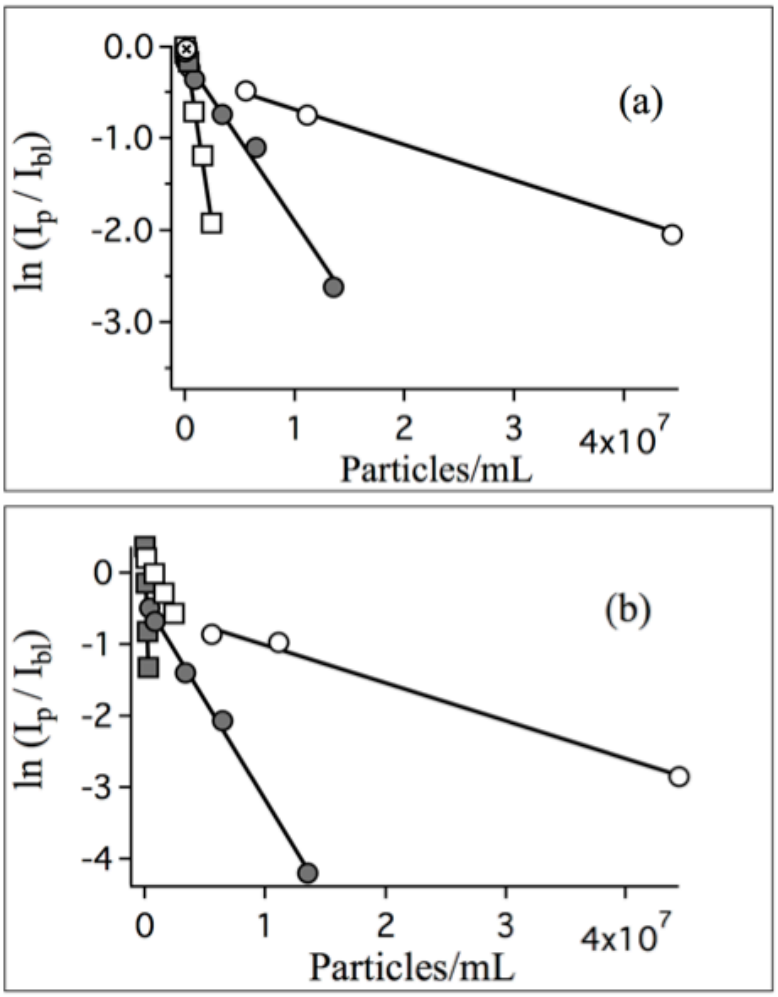

Figure 2.3. Normalized Li intensity verses the total number of monodisperse polystyrene latex particles added to the solution using 532 nm excitation, 0.8 m (○), 2 µm (●), 6 µm (□), 12 µm (■);(a) 500 ppm Li solution and realistic ocean values (⊗).(b) 12.5ppm Li solution

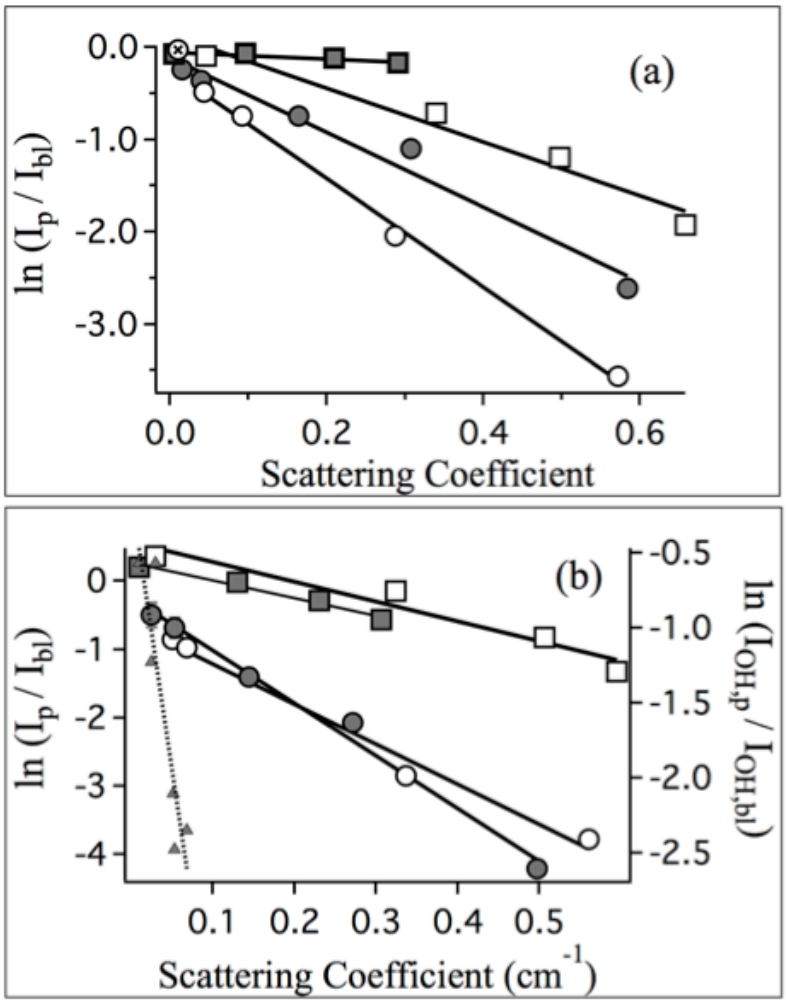

Figure 2.4. Normalized Li LIBS emission verses solution scattering coefficient using 532 nm laser excitation, 0.8 m (○), 2 µm (●), 6 µm (□), 12 µm (■); (a) 500 ppm Li solution and realistic ocean values (⊗). (b) 12.5 ppm Li solution and dotted line showing the stimulated Raman OH-stretch intensity verses scattering coefficient (dotted lines, right axis) for all particle sizes.

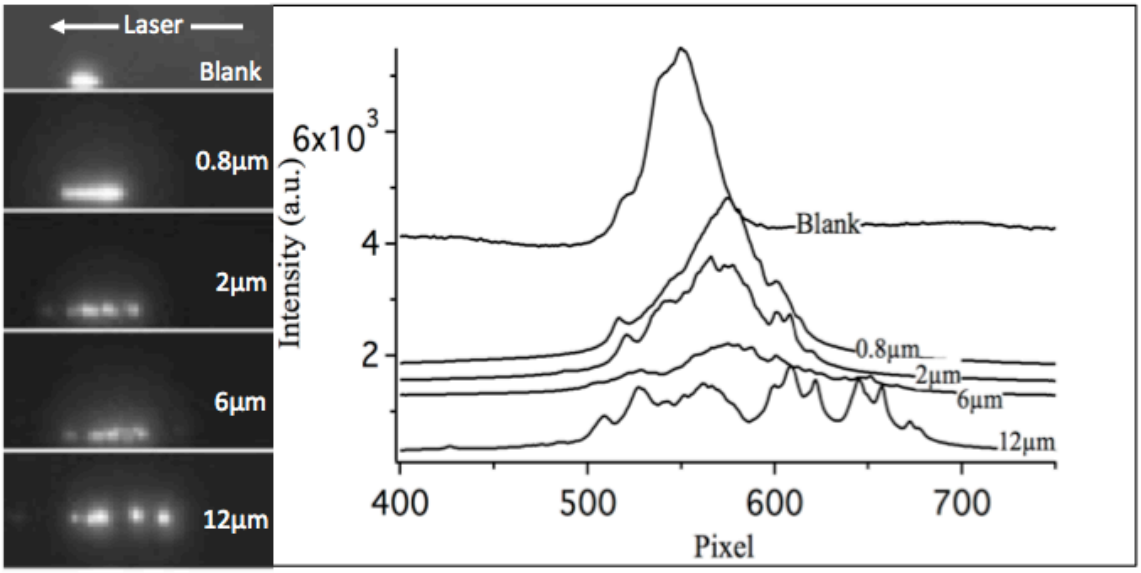

Figure 2.5. Laser wavelength of 532 nm plasma images for each particle size (0.8 µm, 2 µm, 6 µm, and 12 µm) with a scattering coefficient of ~0.245 and lithium concentration of 500 ppm. The plots show column summed cross sections at each particle size

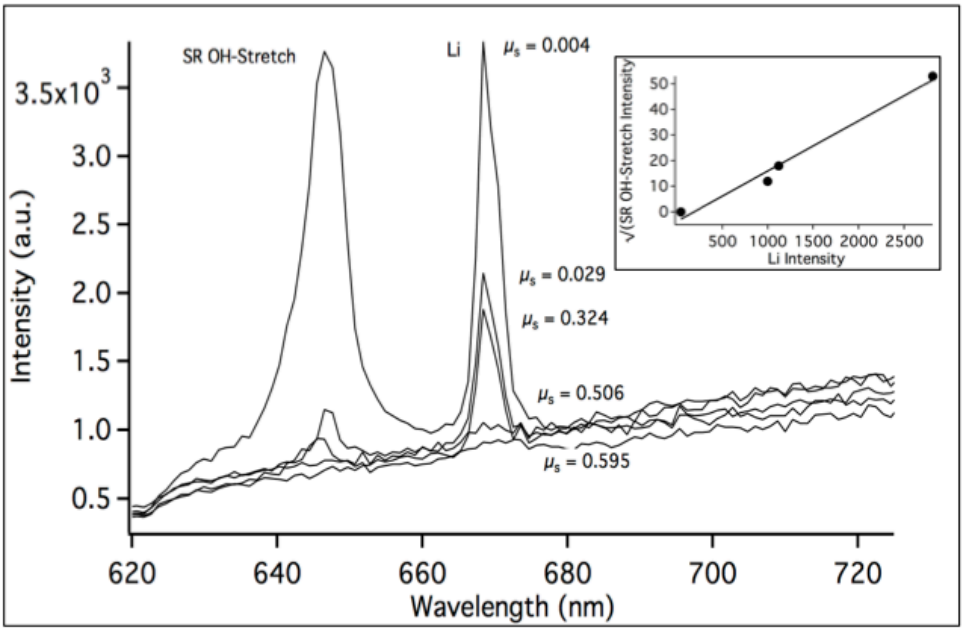

Figure 2.6. Representative spectra for a 12.5 ppm Li solutions with 0.8 µm particles, showing the decrease in Li intensity with increased scattering coefficient, also the appearance of the stimulated Raman OH-stretch peak when using 532 nm excitation and 180˚ collection. Inset shows the stimulated Raman signal decreased as the square compared to the Li emission intensity

CHAPTER 3
HYDROGEN AND OXYGEN AS INTERNAL STANDARDS FOR SINGLE-PULSE LIBS MEASUREMENTS IN BULK AQUEOUS SOLUTIONS

3.1 ABSTRACT

Hydrogen and oxygen line emission is investigated as an internal standard for single-pulse (SP) LIBS measurements of Li and K in bulk aqueous solutions. Simultaneous measurements of hydrogen, oxygen, lithium, and potassium emission lines are made using a short detector delay time and relatively long gate width. These investigations show improved precision in the measured LIBS signal for Li and K using the 656 nm H (α) or the 777 nm O (I) lines as internal standards, with the O (I) line providing up to a 7.5-fold improvement in the relative standard deviation (RSD).

3.2 INTRODUCTION

Laser-induced breakdown spectroscopy (LIBS), first reported by Brech and Cross in 1962 [1], is a relatively simple spectroscopic technique that allows rapid multi-elemental analysis of solids, liquids and gases with little or no sample preparation. LIBS is well suited for *in situ* and remote elemental analysis,[2-20] and is particularly useful for applications in extreme, hostile, and inaccessible environments.[10-18, 21-33] Of particular interest to our research group is using LIBS for multi-elemental analysis of high-pressure

bulk aqueous solutions, with the goal of applying LIBS to *in situ* elemental analysis in the deep ocean,[31-33] particularly at hydrothermal vent sites.

Hydrothermal vents occur at mid-ocean ridges where seawater circulates through the semipermeable ocean crust, exchanging ions along the way. Hot mineral-laden water eventually is expelled at vent orifices at temperatures of 200−405 °C, and at ambient pressures from 8.1×10^6 to 3.6×10^7 Pa, corresponding to ocean depths of 800–3600 m.[34] Conventional analytical measurements of vent fluid is difficult due to high temperatures and pressures at the vent sites, corrosive nature of the vent fluids, difficulty of taking samples at these depths, and irreversible changes in composition that occur when they are removed to the surface.

Aqueous LIBS measurements have been reported for submerged solid materials in water,[16] on the water surface or in thin films,[17–22] and in liquid jets, droplets, and flowing solutions,[23–29] but there are limited reports of LIBS studies in bulk aqueous solutions.[30–32] Pioneering work by Cremers et al. [30] showed that LIBS could be used to identify Li, Na, K, Rb, Cs, Be, Ca, B, and Al in aqueous solutions with varying detection limits, but typically at the parts-per-million level. LIBS measurements of dissolved species in bulk aqueous solution are complicated by water quenching of the LIBS plasma and a reduction in the time during which the plasma emission can be observed as compared to that in air.[16, 30, 31, 33, 40] The plasma lifetime is typically < 1 μs in bulk liquids, whereas at an air–liquid interface it averages 5–20 μs. Laser-induced plasmas formed in solution are also characterized by a reduction in the plasma emission intensity.[31] This leads to reduced measurement precision.

Potentially convenient internal standards for bulk aqueous solution LIBS measurements are hydrogen and oxygen, since these elements are produced by laser decomposition of water during a LIBS measurement, and the density of water in the deep ocean is relatively constant. Fichet, et al, demonstrated the use of H as an internal standard for LIBS surface measurements of a variety of metal species dissolved in water and oil.[18] They also demonstrated the use of O as an internal standard for Al. Samek, et al, also used H as an internal standard for LIBS surface measurements for a range of toxic heavy metals.[38] They also studied the effect of plasma parameters and line shape functions. Mohamed, et al, describe the use of H as an internal standard for LIBS surface measurements for seawater solution.[39] Although using H as an internal standard for LIBS measurements of aqueous solutions has been reported for surface measurements, [18, 38, 39] the use of H or O as internal standards for bulk aqueous LIBS measurements has not been reported. Underwater LIBS is quite different from surface measurements because of rapid water quenching of the LIBS plasma, within a few hundred nanoseconds, and because the spectra are dominated by continuum emission.[40] Thus the behavior of H and O as internal standards might be different for underwater LIBS. In the following studies, the 656 nm hydrogen-α and 777 nm oxygen emission lines are compared as internal standards for LIBS measurements of Li and K for underwater LIBS.

3.3 EXPERIMENTAL

The experimental setup (see Figure 1) used in this study has been previously described,[31-33] and is presented here only briefly. For these experiments a Continuum Surelite III Nd:YAG laser operated at 1064 nm, with a 9 ns pulse width and a repetition

rate of 1-Hz was used for excitation. The laser was directed into the cell by reflection using a 45° dichroic mirror and focused about 1-inch into the solution using a 25-mm diameter, f/2 fused silica lens. Plasma emission was collected and collimated by the same lens, transmitted through the dichroic mirror, and focused by another f/2 lens onto a 2-mm diameter core optical fiber, which was used to direct the emission to an f/4 spectrograph (Chromex Model 250IS/RF) with an ICCD detector. The spectral resolution of the spectrometer was 2.5 nm using a 100-micron slit and a 300 gr/mm diffraction grating, blazed at 1 μm. The ICCD (1024 x 256 pixel, 2D array, Princeton Instruments I-Max 1024-E) gave a spectral range of about 200 nm.

The plasma in bulk water solution is very short-lived and proper detector gating is essential. The detector delay time, t_d, the time at which the detector is turned on following the laser pulse, and the gate width (i.e., exposure time), t_w, the time the detector is on, were optimized to give the strongest emission intensity. The reported emission intensities for all lines are baseline subtracted. The baseline was determined by taking the average value of the baseline at two wavelengths on either side of the line of interest. Solutions were made, by dissolving LiCl and KCl (Sigma-Aldrich ACS certified, 99%, and 99.42% purity, respectively) in 17.7MΩ deionized water. All concentrations are given in parts per million (mass/volume). All measurements were made ~1-in below the surface in bulk aqueous solution. Relative standard deviation (RSD) values were calculated using three sets of 200, single-shot spectra.

3.4 Results and Discussion

Lithium is normally found in the ocean at trace levels, below 1 ppm.[34] However, localized high concentrations of Li associated with hydrothermal vent sites can be in the 10s of ppm, because of leaching from rocks by the hot vent fluids.[35] Thus Li is a useful tracer of vent fluids and is useful to map their extent. Potassium at ~400 ppm, is the sixth most abundant element in seawater. It has a conservative distribution, its concentration varying due to differences in evaporation or precipitation in surface water that sinks to deeper waters. Large changes in potassium concentrations at vent sites have been shown to be associated with phase separation events with concentrations over 2000 ppm reported.[35-37]

Figure 2 shows the LIBS spectrum of a solution that contains ~50 ppm Li and ~1000 ppm K. The Li and K emission lines are observed at 671 nm and 766 nm, respectively. Table 3.1 shows the observed wavelength, transition probabilities (A_{ki}), and upper (E_k) and lower (E_i) state energies for the Li, K, H and O lines used in this study (taken from NIST Atomic Spectra Database)**.** Note the Li and K transitions are to the ground state, while H and O emission is to a very high-energy state. The LIBS emission for these two Li and K lines is strong; however, the LIBS emission intensity varies as much as 15% from shot-to-shot. This large variation is partly the result of laser shot-to-shot power fluctuations. It is also the result of large variations in the size, location and intensity of the underwater LIBS plasma. Changes in the plasma properties from shot-to-shot effects the width of the H(α) emission line, as shown below. Figure 3 shows two different Li calibration curves, for solutions containing 1000 ppm K and Li at concentrations ranging from 1.7 to 53 ppm. One plot (solid line, open circles) shows the

raw emission intensity (left axis) and the other plot (dashed line, open triangles) shows the ratio of Li emission to K emission (right axis). The residuals are shown at the bottom of the figure (solid line Li, dashed line Li/K ratio). As expected, the precision of the Li/K ratio is better than Li emission alone. However, for LIBS measurements of deep-ocean hydrothermal vent fluids, it is desirable to have an internal standard with a fixed or known concentration.

To be useful as an internal standard, H and O emission should be measured simultaneously with the analyte. However, H and O emission in solution is very short lived relative to Li and K.[31] The high-energy H and O lines are quenched much more quickly than Li emission in water, requiring a very short detector gate delay, compared to Li. Figure 4 (top) shows the LIBS emission lines for H (656 nm) and O (777 nm) in 25 ppm Li solution at 1 Bar and 300 Bar using a 192 ns gate delay with a 1 μs gate width. The lower spectrum was measured similarly for a K solution at 1 Bar. The combination of a short detector gate delay with a wide width allows the short H and O lines to be measured simultaneously with the Li or K emission. Figure 5 shows the time profile of these H, O and Li emission lines. The emission of the H and O lines reaches a maximum at ~120-140 ns after the laser pulse, then decays quickly, while Li emission is not observed at all at ~125 ns, reaching a maximum at ~175-200 ns. The time profiles are similar for K and for solution pressures up to 300 Bar.

Figure 6 shows Li (top) and K (lower) calibration curves up to 500 ppm plotted as Li and K emission intensity (open squares), Li/H and K/H intensity ratios (open circles), and Li/O and K/O intensity ratios (open triangles). These measurements were made using a laser energy of 192 mJ per pulse, and each measurement is the average of 200 laser

shots. Measurements were made in triplicate and the error bars show plus or minus one standard deviation. The Li/H and Li/O ratios both track the Li intensity well, with the Li/O ratio showing lower variability between measurements at a given concentration than the Li/H ratio. The K/O ratio tracks the K emission well with significantly improved variability between measurements at a given concentration. However, the K/H ratio did not track the K emission intensity well and showed relatively poor reproducibility between measurements.

In a study to compare the variability for single-shot LIBS measurements of the Li emission intensity with the Li/H and Li/O ratios, and the K emission intensity with the K/H and K/O ratios, the standard deviations of the Li and K emission intensities for 200, single-shot LIBS spectra were calculated. The sets of 200-shot measurements were done in triplicate and the pooled standard deviation for all 600 shots was used to calculate the relative standard deviation of the emission intensity, and the H and O intensity ratios for Li and K. This was done for different Li and K concentrations and laser pulse energies. The RSD results are tabulated for 5 ppm Li and 100 ppm K solutions in Table 3.2 and Table 3.3, respectively. At any specific concentration it was found that the RSDs of the H and O ratios were lower for both Li and K, at all laser pulse energies used. The O ratio worked better than the H ratio for both elements. In the case of Li, the lowest Li/O RSD was 2%, improved up to 7.5-fold compared to the RSD of the Li intensity alone. The maximum Li/H improvement in the RSD was 6%, a ~2-fold improvement compared to the RSD of the Li intensity alone. In the case of K, the lowest Li/O RSD was 4%, a ~3-fold improvement compared to the RSD of the K intensity alone. There was little improvement using the K/H ratio. The H(α) line is very broad due to Stark broadening

and the width of this line varied considerably from shot to shot in this study, on the order of 8%. The O line is relatively narrow and the width varied only about 4%. Because of the broadness of the H line and the variability in its width, the H intensity was sometimes difficult to determine. This lead to a larger variation in the Li/H and K/H ratios and larger RSD values compared to the Li/O and K/O ratios.

Figure 7 shows the RSD for Li emission intensity at three different concentrations, compared to the Li/H and Li/O emission intensity ratios. While there was some variation in the Li RSD with concentration, the ratio measurements did not vary much with concentration. A similar result was seen for K.

As shown in Tables 3.2 and 3.3, the RSD of all measurements improved as the laser pulse energy was increased. On the other hand, the intensity of all of the emission lines decreased exponentially with increasing pulse energy as shown in Figure 8. This effect could be the result of plasma shielding, potentially an issue using the 180º backscatter configuration. The larger effect for the H and O lines compared to Li and K emission is consistent with increasing electronic temperature at higher laser power, leading to reduced concentrations of neutral species. The much higher ionization energy of H and O might lead to a larger relative change in neutral species concentrations as the laser power is increased. At the higher laser power the H and O emission intensity is very insensitive to changes in laser power. This could explain why the RSD values were lower at higher laser power.

3.5 Conclusions

Hydrogen and oxygen emission can be measured simultaneously with Li and K emission using LIBS in bulk aqueous solution, up to 300 bar pressure. Calibration plots using Li/H, Li/O, K/H, and K/O emission ratios track the Li and K emission intensity calibration curves very well. As internal standards, H and O both improve the precision of replicate Li and K measurements, with the O ratio showing the largest improvement. The biggest improvement is seen at the higher laser pulse energies tested, even though emission of all species decreased with increasing laser pulse energy.

3.6 References

1. Brech, F.; Cross, L., Optical microemission simulated by a ruby maser, Appl. Spectrosc., 1962. 16; 59.

2. Majidi V.; Joseph, M.; Spectroscopic applications of laser induced plasmas, Crit. Rev. Anal. Chem. 1992. 23; 143–162.

3. Radziemski, L.; Cremers, D.A.; Benelli, K.; Khoo, C.; Harris, R.D.; Use of the vacuum ultraviolet spectral region for laser-induced breakdown spectroscopy-based Martian geology and exploration, Spectrochim. Acta Part B 2005. 60: 237-248.

4. Rusak, D.; Castle, B.; Smith, B.; Winefordner, J.; Fundamentals and applications of laser-induced breakdown spectroscopy, Crit. Rev. Anal. Chem., 1997. 27; 257–290.

5. Song, K.; Lee, Y.; Sneddon, J.; Applications of laser-induced breakdown spectrometry, Appl. Spectrosc. Rev. 1997. 32; 183–235.

6. Sneddon, J.; Lee, Y.; Novel and recent applications of elemental determination by laser-induced breakdown spectroscopy, Anal. Lett. 1999. 32; 2143–2162.

7. Rusak, D.; Castle, B.; Smith, B.; Winefordner, J.; Recent trends and the future of laser-induced plasma spectroscopy, Trend. Analyt. Chem. 1998. 17: 453–461.

8. Lee W.; Wu J.; Lee Y.; Sneddon J.; Recent applications of laser-induced breakdown spectrometry: a review of material approaches, Appl. Spectrosc. Rev., 2004. 39; 27–97.

9. Salle, B.; Lacour, J.L.; Vors, E.; Fichet, P.; Maurice, S.; Cremers, D. A.; Wiens R. C., Laser-induced breakdown spectroscopy for Mars surface analysis: capabilities at stand-off distances and detection of chlorine and sulfur elements, Spectrochim. Acta Part B, 2004. 59: 1413–1422.

10. Arp, Z.; Cremers, D.; Harris, R. D.; Oschwald, D.; Parker, G.R. Jr.; Wayne, D.; Feasibility of generating a useful laser induced breakdown spectroscopy plasma on rocks at high pressure: preliminary study for a Venus mission, Spectrochim. Acta Part B 2004. 59; 987–999.

11. Seyfried, W. Jr.; Johnson, K.; Tivey, M. C.; In-situ sensors: their development and application for the study of chemical, physical and biological systems at mid-ocean ridges, NSF_Ridge Sponsored Workshop Report (2000).

12. The next generation of in situ biological and chemical sensors in the ocean: a workshop report, (2004).
URL:http://www.whoi.edu/institutes/OLI/activities/symposia_sensors.htm.

13. Daly, K.; Byrne, R.; Dickson, A.; Gallager, S.; Perry, M.; Tivey, M.; Chemical and biological sensors for time-series research: current status and new directions, Mar. Technol. Soc. J., 2004. 38; 121–143.

14. Dickey, T.; The role of new technology in advancing ocean biogeochemical studies, Oceanography 2001. 14: 108–120.

15. Varney, M.; ed., Chemical Sensors in Oceanography (Gordon and Breach, 2000).

16. Pichahchy, A.; Cremers, D.; Ferris, M.; Elemental analysis of metals under water using laser-induced breakdown spectroscopy, Spectrochim. Acta Part B, 1997. 52; 25–39.

17. Fichet, P.; Menut, D.; Brennetot, R.; Vors, E.; Rivoallan, A., Analysis by laser-induced breakdown spectroscopy of complex solids, liquids, and powders with an echelle spectrometer, Appl. Optics. 2003. 42; 6029-6035.

18. Fichet, P.; Mauchien, P.; Wagner, J.F.; Moulin, C.; Quantitative elemental determination in water and oil by laser induced breakdown spectroscopy, Anal. Chim. Acta 2001. 429; 269–278.

19. Arca, G.; Ciucci, A.; Palleschi, V.; Rastelli, S.; Tognoni, E.; Trace element analysis in water by the laser-induced breakdown spectroscopy technique, Appl. Spectrosc. 1997. 51 1102–1105.

20. Samek, O.; Beddows, D.; Kaiser, J.; Kukhlevsky, S.; Liska, M.; Telle, H. H.; Young, J.; Application of laser-induced breakdown spectroscopy to in situ analysis of liquid samples, Opt. Eng. 2002. 39; 2248-2262.

21. Paksy, L.; Német, B.; Lengyel, A.; Kozma, L.; Czekkel, J.; Production control of metal alloys by laser spectroscopy of the molten metals. Part 1. Preliminary investigations, Spectrochim. Acta Part B, 1996. 51; 279-290.

22. Tran, M.; Sun, Q.; Smith, B.; Winefordner, J.D.; Direct determination of trace elements in terephthalic acid by laser induced breakdown spectroscopy, Anal. Chim. Acta, 2000. 419; 153-158.

23. Wainner, R.T.; Harmon, R.S.; Miziolek, A.W.; McNesby, K.L.; French, P.D.; Analysis of environmental lead contamination: comparison of LIBS field and laboratory instruments, Spectrochim. Acta Part B, 2001. 56; 777-793.

24. Barbini, R.; Colao, F.; Lazic, V.; Fantoni, R.; Palucci, A.; Angelone, M.; On board LIBS analysis of marine sediments collected during the XVI Italian campaign in Antarctica, Spectrochim. Acta Part B, 2002. 57; 1203-1218.

25. Bulajic, D.; Cristoforetti, G.; Corsi, M.; Hidalgo, M.; Legnaioli, S.; Palleschi, V.; Salvetti, A.; Tognoni, E.; Green, S.; Bates, D.; Steiger, A.; Fonseca, J.; Martins, J.; McKay, J.; Tozer, B.; Wells, D.; Wells, R.; Harith, M.A.; Diagnostics of high-temperature steel pipes in industrial environment by laser-induced breakdown spectroscopy technique: the LIBSGRAIN project, Spectrochim. Acta Part B 2002 57 1181-1192.

26. Noda, M.; Deguchi, Y.; Iwasaki, S.; Yoshikawa, N.; Detection of carbon content in a high-temperature and high- pressure environment using laser-induced breakdown spectroscopy, Spectrochim. Acta Part B 2002. 57; 701-709.

27. Lee W.; Wu J.; Lee Y.; Sneddon J.; Recent applications of laser-induced breakdown spectrometry: a review of material approaches, Appl. Spectrosc. Rev., 2004. 39; 27–97.

28. Munson, C.A.; De Lucia F.C. Jr.; Piehler, T.; McNesby, K.L.; Miziolek, A.W.; Investigation of statistics strategies for improving the discriminating power of laser-induced breakdown spectroscopy for chemical and biological warfare agent simulates, Spectrochim. Acta Part B, 2005. 60; 1217-1224.

29. Sallé, B.; Cremers, D.A.; Maurice, S.; Wiens, R.C.; Laser-induced breakdown spectroscopy for space exploration applications: Influence of the ambient pressure on the calibration curves prepared from soil and clay samples, Spectrochim. Acta Part B 2005. 60: 479-490.

30. Cremers, D.A., L.J. Radziemski, T.R. Loree, Spectrochemical analysis of liquids using the laser spark, Appl. Spectrosc., 1984. 38; 721-729.

31. Lawrence-Snyder, M.; Scaffidi, J.; Angel, S. M.; Michel, A.P.M.; Chave, A.D.; Laser-Induced Breakdown Spectroscopy of High-Pressure Bulk Aqueous Solutions, Appl. Spectrosc. 2006. 60; 786-790.

32. Lawrence-Snyder, M.; Scaffidi, J.; Angel, S.M.; Michel, A.;Chave, A. Sequential-Pulse Laser –Induced Breakdown Spectroscopy of High-Pressure Bulk Aqueous Solutions, Appl. Spec., 2007. 61; 171-176.

33. Michel, A.; Lawrence-Snyder, M.; Angel, S.M.; Chave, A., Laser-induced breakdown spectroscopy of bulk aqueous solutions at oceanic pressures: evaluation of key measurement parameters, Appl. Optics. 2007. 46; 2507-2515.

34. Seyfried, W.E., Jr.; Janecky D.R.; Mottl, M.J.; Alteration of the oceanic crust: Implications for geochemical cycles of lithium and boron, Geochimica Acta, 1984. 48; 557-569.

35. German, C.R.; Von Damm, K.L.; Hydrothermal processes Treatise on Geochemistry, H. Elderfield, H. D. Holland, and K. K. Turekian, eds. Elsevier. 2003. 6; 181-222.

36. Tivey, M.; Generation of Seafloor Hydrothermal Vent Fluids and Assocated Mineral Deposits, Oceanography. 2007. 20; 50-65.

37. Von Damm, K.L.; Lilley, M.D.; Shanks W.C. III; Brockington, M.; Bray, A.M.; O'Grady, K.M.; Olson, E.; Graham, A.; Proskurowski G.; SouEPR Science Party, Extraordinary phase separation and segregation in vent fluids from the southern East Pacific Rise, E. Pl. Sci. Lett., 2003. 206; 365-378.

38. Samek, O.; Beddows, D.; Kaiser, J.; Kukhlevsky, S.; Liska, M.; Telle, H. H.; Young, J.; Application of laser-induced breakdown spectroscopy to in situ analysis of liquid samples, Opt. Eng. 2002. 39; 2248-2262.

39. Mohamed, W.T.Y.; Quantitative elemental analysis of seawater by laser induced breakdown spectroscopy, Int, J. Pure Appl. Phys. 2006. 2; 11-21.

Table 3.1. Observed wavelength, transition probabilities (A_{ki}), and upper (E_k) and lower (E_i) state energies for the Li, K, H and O lines used in this study (taken from NIST Atomic Spectra Database).

Element	Wavelength (nm)	A_{ki} (s^{-1})	E_i (cm^{-1})	E_k (cm^{-1})
H	656.2819	4.41E+07	82259.158	97492.304
O	777.1944	3.69E+07	73768.2	86631.454
Li	670.776	3.69E+07	0	14904
K	766.48	3.80E+07	0	13042.896

Table 3.2. RSD values of the 671 nm Li line intensity, the Li/H emission ratio and the Li/O emission ratio for triplicate measurements of 200, single-shot LIBS spectra, for 5 ppm Li, measured at 145 mJ, 166 mJ, 192 mJ, 222 mJ, and 260 mJ laser pulse energy.

Lithium Concentration 5 ppm					
Laser Power	145 mW	166 mW	192 mW	222 mW	260 mW
Li Signal RSD	0.24	0.22	0.15	0.14	0.13
Li Signal Ratioed to H Signal RSD	0.16	0.15	0.09	0.06	0.08
Li Signal Ratioed to O Signal RSD	0.10	0.03	0.02	0.03	0.02

Table 3.3. RSD values for triplicate measurements of 200 laser shots each, of K emission, the K/H emission ratio and the K/O emission ratio for 100 ppm K, measured at 145 mJ, 166 mJ, 192 mJ, 222 mJ, and 260 mJ laser pulse energy.

Potassium 100 ppm					
Laser Power	145 mW	166 mW	192 mW	222 mW	260 mW
K Signal RSD	0.24	0.19	0.13	0.11	0.10
K Signal Ratioed to H Signal RSD	0.18	0.18	0.17	0.12	0.09
K Signal Ratioed to O Signal RSD	0.17	0.08	0.07	0.04	0.08

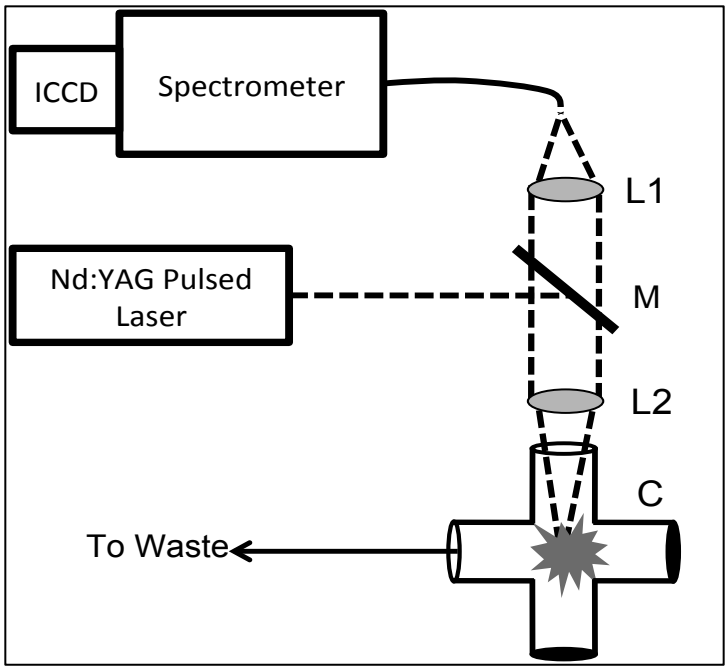

Figure 3.1. Experimental laser induced breakdown spectroscopy set-up for the studies of hydrogen and oxygen as internals standards. L1 & L2 are f/2 plano convex lenses, M is a dichroic mirror, C is the sample cell.

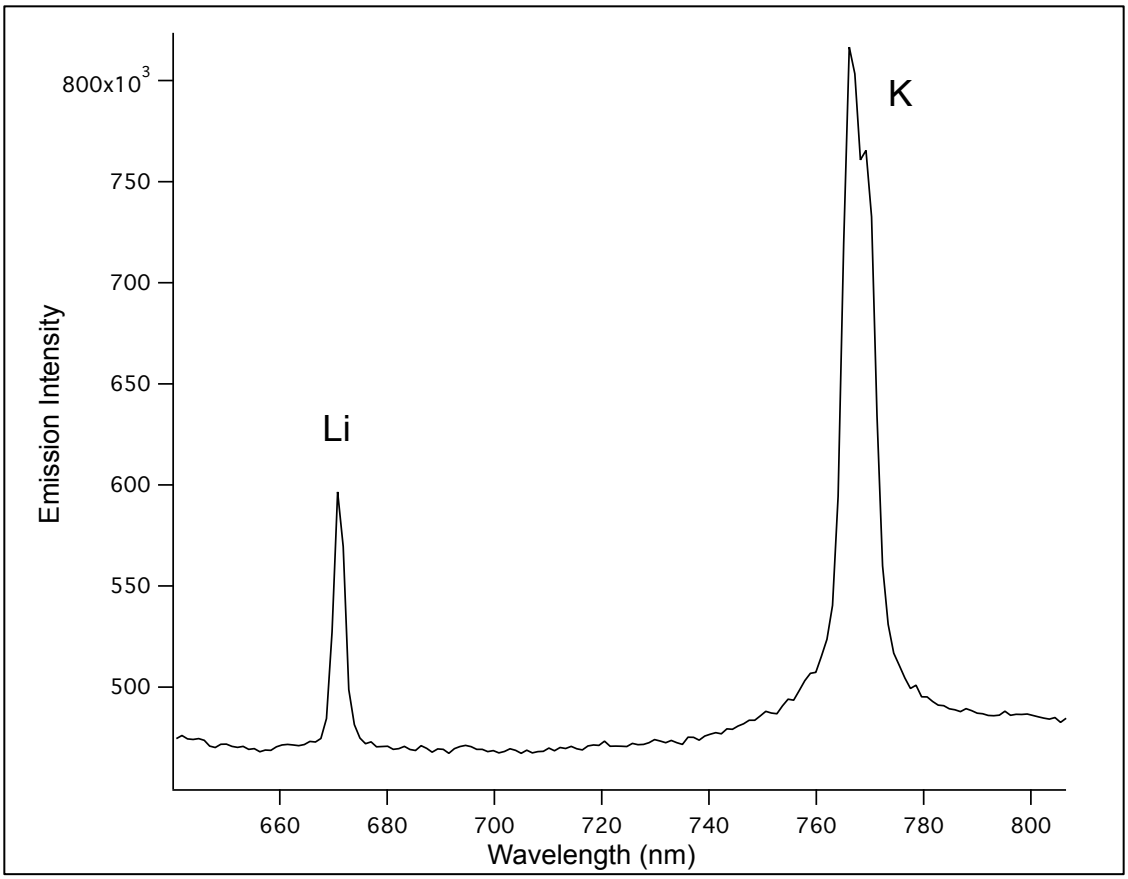

Figure 3.2. Bulk aqueous solution, SP LIBS spectrum of a solution containing ~50 ppm Li and ~1000 ppm K measured using a 1064 nm pulsed laser.

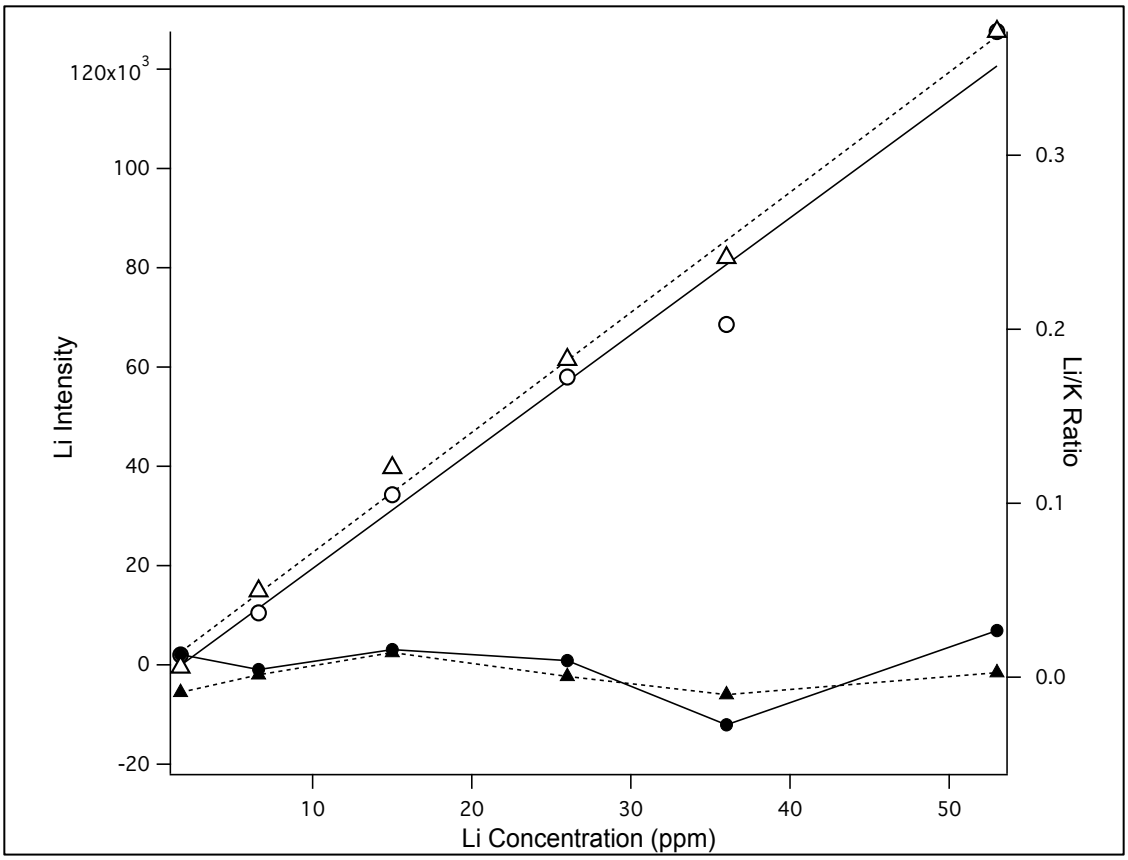

Figure 3.3. Calibration curves for Li, plotted as Li emission (open circles, solid line) and as the Li/K ratio (open triangles, dashed line) where the K concentration was 1000 ppm for all solutions. The residuals are also plotted, for Li emission (closed circles, solid line) and the Li/K ratio (closed triangles, dashed line).

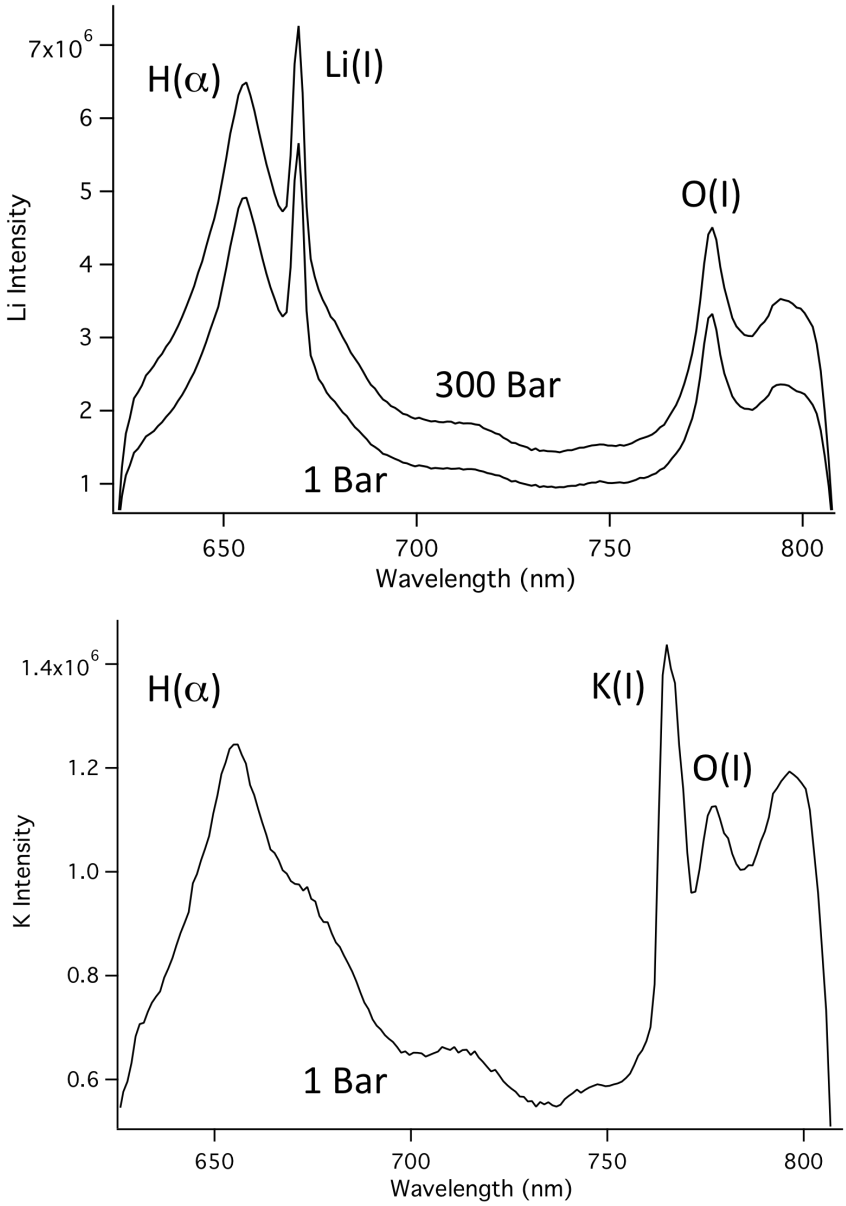

Figure 3.4. Bulk aqueous solution, SP LIBS spectra of a 25 ppm Li solution at 1 Bar and 300 Bar pressure (Top), and a 100 ppm K solution at 1 Bar. The detector gate delay and gate width were 192 ns and 1 ms, respectively.

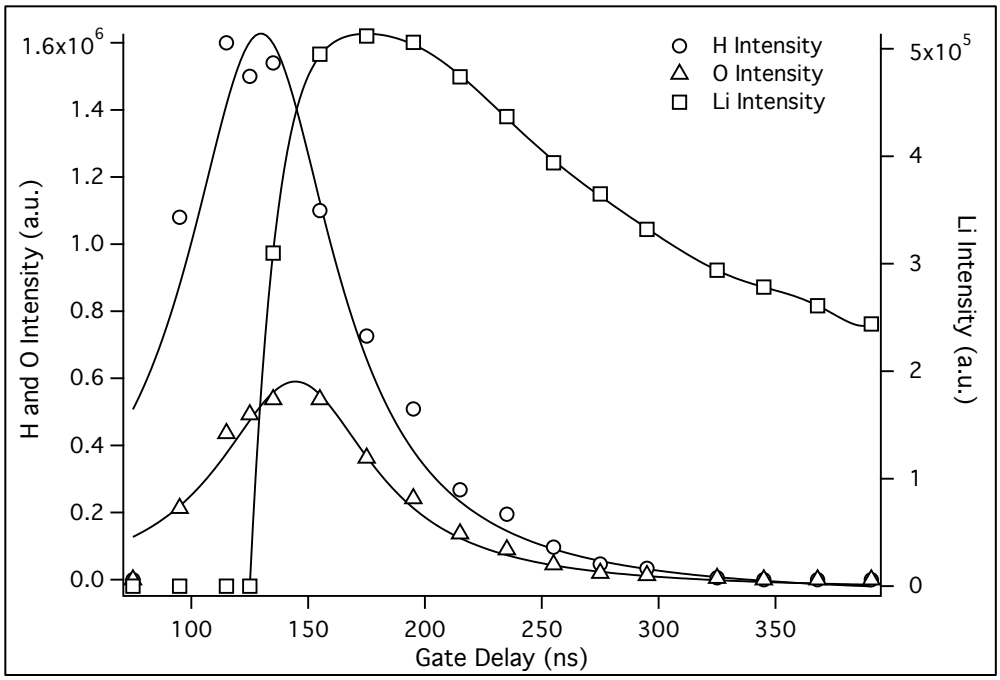

Figure 3.5. Plots of emission intensity versus gate delay for the 671 nm Li, 656 nm H and 777 nm O lines measured using a 5 ppm Li solution.

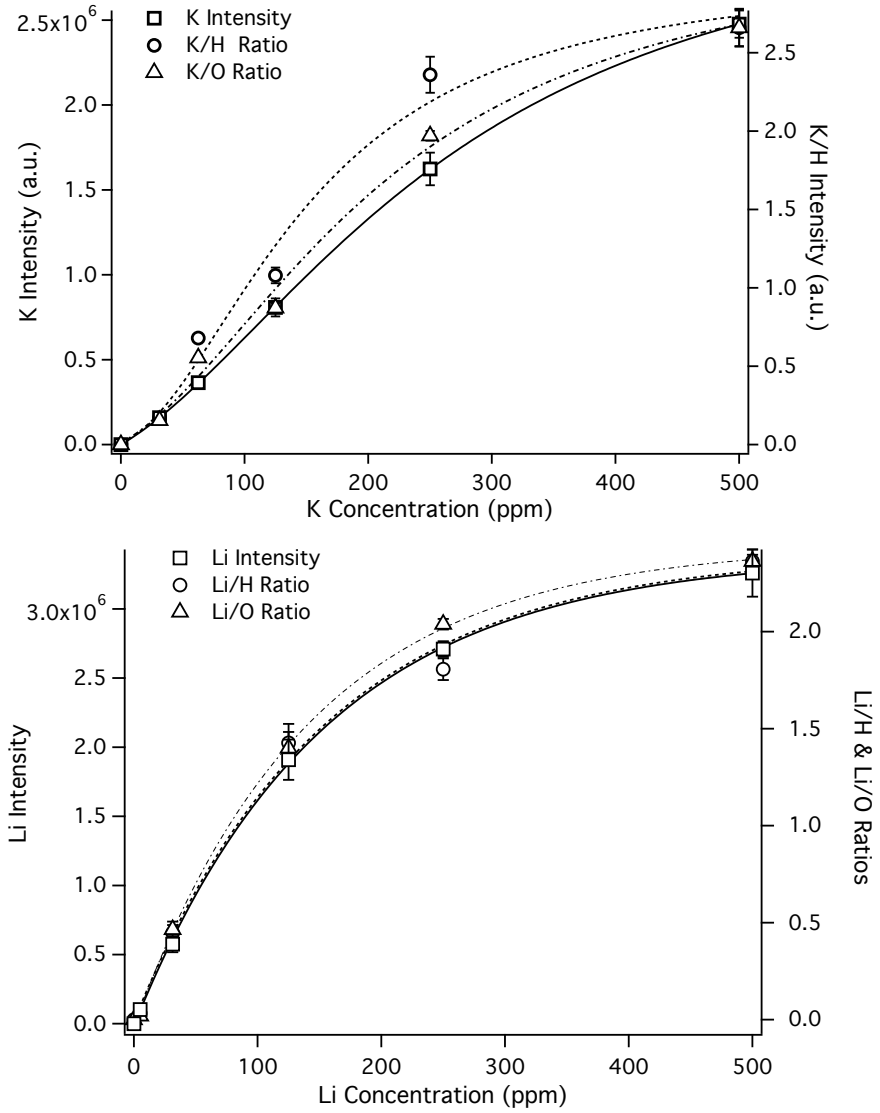

Figure 3.6. Calibration curves for Li (top) and K (lower) solutions using the 671 nm Li and 766 nm K emission line intensities and the Li/H and Li/O intensity ratios (top) and K/H and K/O intensity ratios (lower), using 192 mJ per pulse. Error bars show ±1 standard deviation for triplicate measurements.

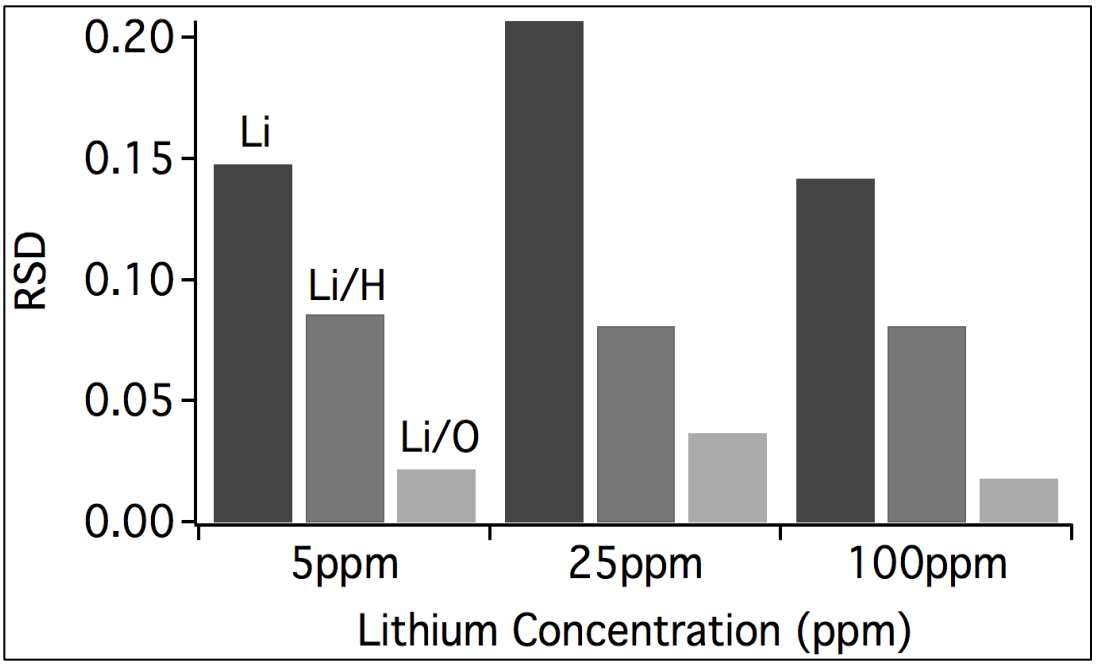

Figure 3.7. RSD values for lithium emission (Li) and the Li/H and Li/O ratios for 5 ppm, 25 ppm and 100 ppm Li solutions, using 192 mJ per pulse laser energy. The RSD values were calculated based on the standard deviation of the intensity for 200, single-shot measurements. The RSD was calculated by pooling the standard deviation for three sets of 200-shots.

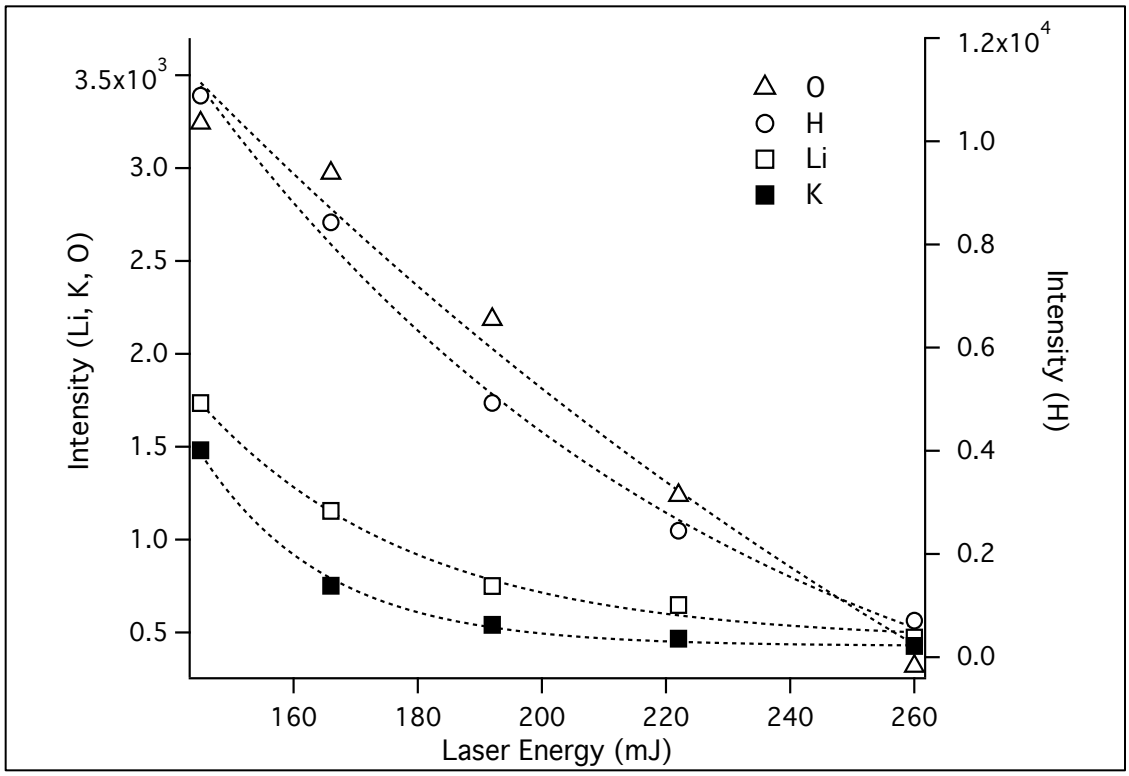

Figure 3.8. Emission intensity for the 671 nm Li (open squares), 766 nm K (filled squares), 656 nm H(α) (open circles) and 777 nm O (open triangles) lines, versus laser pulse energy, for a solution containing 5 ppm Li and 25 ppm K.

CHAPTER 4
DESIGN AND TESTING OF A SUPER CRITICAL CO_2 CELL

4.1 INTRODUCTION

Mars and Venus are the two bodies in our solar system that are most similar to Earth, however Mars has little to no atmosphere and Venus has the most powerful greenhouse effect found in the solar system, which makes them ideal to study.[1] The National Aeronautics and Space Administration (NASA) has landed four different rovers on the surface of Mars, with the most recent being the Mars Science Laboratory rover Curiosity. ChemCam on Curiosity is the first LIBS instrument to be operated on another planet and is capable of sample analysis up to 7 m away.[1-4] The success of this instrument has aided in the idea of using LIBS for other planetary missions such as on the surface of Venus.

Venus has dense clouds above the surface that makes orbital surveys difficult requiring the need for a lander mission. Missions to Venus using a rover that lands on the surface will be no easy feat due to the extremely harsh environment. The Venusian atmosphere is 97% CO_2 with a surface pressure of 90 bars and surface temperature of ~735K. This causes the CO_2 to be in a super critical state (P >72.9 bar, T >304.25 K) at the surface.[1,2] While Venus has many similarities in size, mass, and the amount of solar energy from the sun, there is a significant difference in the surface conditions. These

differences drive scientist to want to better understand why Venus is the planet it is today.[4]

Soviet Venusian surface probes have had an operational lifetime of ~2 hours. A LIBS instrument has several key characteristics that make it suitable for measurements under the extreme environmental conditions of Venus. LIBS is standoff capable allowing it to perform from the safety of the lander. Eliminating the risks of drilling, collecting, delivering a sample with a contact instrument. LIBS is also able to make several thousand measurements of the surrounding landing site during the lifetime of a Venus lander.

LIBS has been proposed for measurements on Venus before, however when forming the plasma in supercritical CO_2 there will be a refractive index change and it will interfere with the emission. Therefore, a supercritical CO_2 setup has been designed and build to make measurements under these conditions.

4.2 EXPERIMENTAL

Figure 4.1 illustrates the experimental setup for super critical CO_2 measurements. For safety of the operator, a containment chamber was built around the entire setup using 3/4" thick ultra impact resistant clear polycarbonate (McMaster-Carr, 84805K32). In order to produce super critical CO_2 all the valves (V) start in the closed position. The high-pressure cell is wrapped in heat tape and set to a temperature of 50 C˚ (Brisk Heat, SDC120JC-A) and allowed to equilibrate for ~5 hours. The CO_2 cylinder is opened. The pressure exiting the cylinder is ~52 atm, which is less then the pressure need to be super critical, therefore a high pressure pump is utilized. For all measurements V_4 was opened so the 100 atm blow off valve was being used and not the 290 atm blow off. The high-

pressure cell is initially charged to ~52 atm by opening V_1. Once the pressure reaches ~52 atm then V_1 is closed isolating the sample cell. V_2 is then opened and the pump is filled with CO_2. V_2 is then closed and V_3 is opened so the pump can increase the pressure of the cell to a pressure <80 atm.

All measurements were made using a Continuum Surelite III Nd:YAG laser for excitation operated at 1064 nm with a repetition rate of 1 Hz. The laser was directed into a custom stainless steel cell with 25.4 mm dia x 6.35 mm thk sapphire windows (Meller Optics Inc., SCD3789-02B) and PTFE seals (1.6 mm thk), by reflection from a 45° dichroic mirror (DM) and focused into the super critical CO_2 using a 25.4 mm diameter, f/2 fused silica lens (L_1). LIBS emission was collected back through the same lens and focused using a second 25.4 mm diameter f/2 lens (L_2) on to a 2 mm core diameter optical fiber, which was coupled to a f/4 dispersive spectrometer (Chromex Model 250IS/RF) with 600 gr/mm grating blazed at 750 nm, which allowed for a ~95 nm spectral window and resolution of ~1.5 nm. The collection system consisted of a gated 1064x256 pixel ICCD (Princeton Instruments I-Max 1024-E).

4.3 Results and Discussion

Figure 4.2 shows shadowgraph images of the laser induced plasma formed in super critical CO_2 at a pressure of 85 atm and temperature of 40 ˚C, at t_d= 350 ns, as well as the formation of a cavitation bubble formed starting at a later time and finally collapsing at 5 μs. These results are similar to what is seen in shadowgraph images in bulk aqueous solution under pressure.[5] Figure 4.3 shows a LIBS spectrum of supercritical CO_2 showing the strong 777 nm oxygen(I) line. In Figure 4.4 shows the

supercritical CO_2 cell, which has been wrapped in heat tape with an olivine sample. The olivine sample was held in place in the cell using an 18/10 stainless steel spring clamp. Figure 4.5 shows the LIBS spectrum of olivine in super in supercritical CO_2 at 80 atm and 40 C°, relevant to measurements of minerals on Venus. This spectrum was stitched together from 9 separate spectra, since the spectrometer spectral window was only ~95 nm. The more intense lines were assigned using NIST Atomic spectral database.

One of our interests is possible pressure effects on the LIBS emission. Figure 4.6 shows that in the pressure range of 73 to 120 atm there are no significant pressure effects on the position and width of the, 767 nm, 778 nm, and 781 nm Fe lines. These initial tests on the new supercritical CO_2 LIBS emission cell do not show any issues related to large changes in refractive index, or cloudiness when the plasma was formed in supercritical CO_2, however, further studies need to be done.

4.4 REFERENCES

1. Moroz, V.I.; Studies of the atmosphere of Venus by means of spacecraft: Solved and unsolved problems, Adv. Space Res., 2002. 29; 215-225.

2. Clegg, S.; Wiens, R.; Misra, A.; Sharma, S.; Lambert, J.; Bender, S.; Mewell, R.; Nowak-Lovato, K.; Smrekar, S.; Dyar, M.; Maurice, S.; Planetary Geochemical investigations Using Raman and Laser-Induced Breakdown Spectroscopy, Appl. Spec., 2014. 68; 925-936.

3. Sharma, S.; Misra, A.; Singh, U.; Remote Raman Spectroscopy of Minerals at Elevated Temperature Relevant to Venus Exploration, SPIE 7153, Lidar Remote Sensing for Environmental Monitoring IX, 8 December 2008; doi: 10.1117/12.806371.

4. Sharma, S.; Misra, A.; Clegg, S.; Barefield, J.; Weins, R.; Acosta, T.;Time-resolved remote Raman study of minerals under supercritical CO2 and high temperatures relevant to Venus exploration, Phil. Trans. R. Soc. A, 2010. 368; 3167-3191.

5. Angel, S.M.; Bonvallet, J.; Lawrence-Snyder, M.; Pearman, W.F.; Register, J.; Underwater measurements using laser induced breakdown spectroscopy. J. Anal. At. Spectrom., 2016. 31; 328-336.

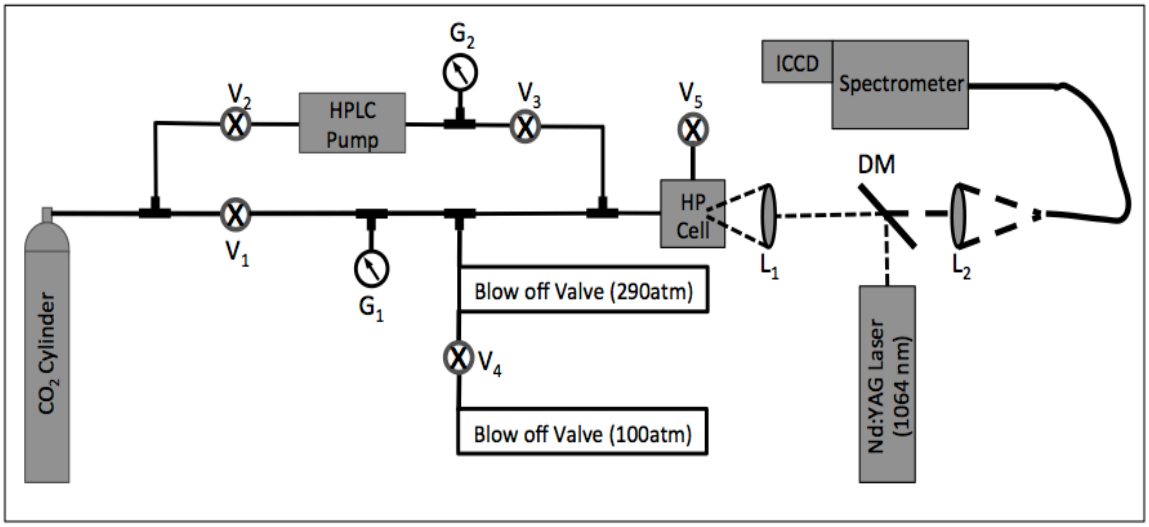

Figure 4.1. Experimental set up for super critical CO_2 measurements.

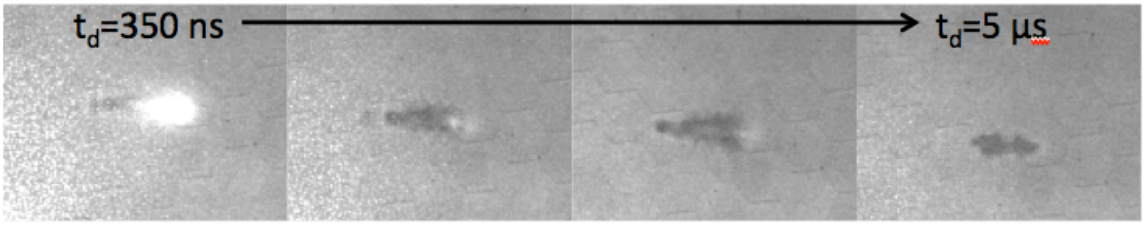

Figure 4.2. Shadowgraph images of the plasma and cavitation bubble formation in supercritical CO_2 (T= 40 C˚, P= 85 atm)

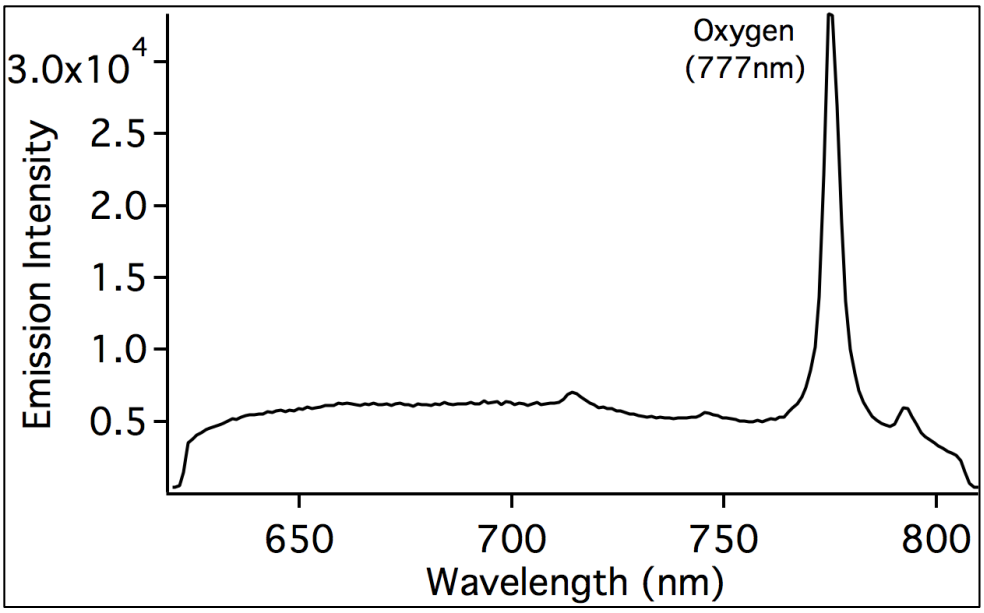

Figure 4.3. Spectrum of supercritical CO_2, with a strong oxygen emission at 777 nm.

Figure 4.4. Supercritical CO_2 cell wrapped in heat tape with a piece of olivine held in the center.

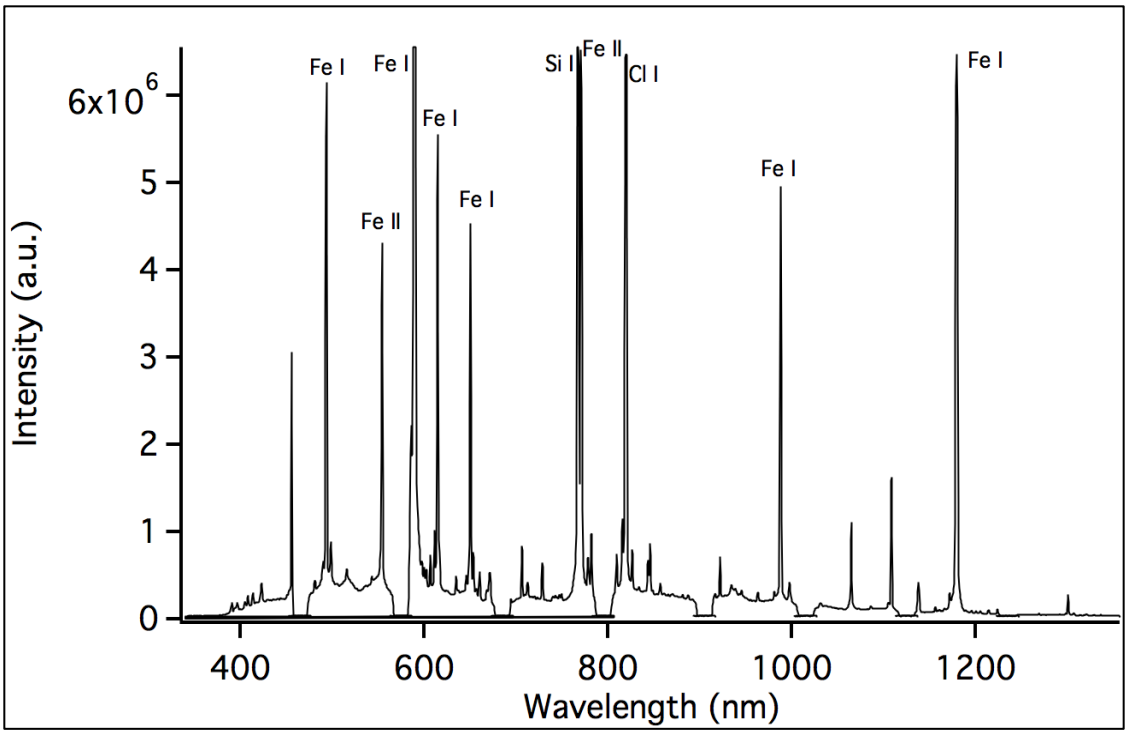

Figure 4.5. Spectrum of the mineral olivine

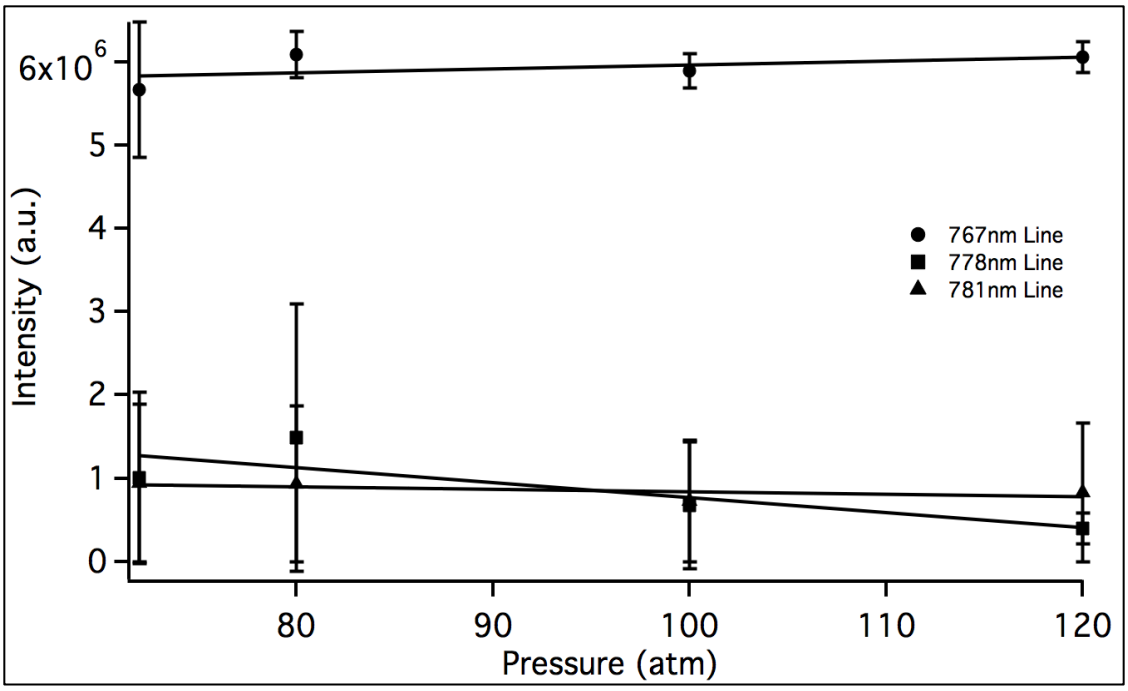

Figure 4.6. Plot of Fe line (767 nm, 778 nm, 781 nm) intensities in olivine as a function of pressure.

REFERENCES

Ahmed, R.; Baig, A.; A comparative study of single and double pulse laser induced breakdown spectroscopy, J. Appl. Phys. 2009. 106; 033307-1-033307-6.

Angel, S.M.; Bonvallet, J.; Lawrence-Snyder, M.; Pearman, W.F.; Register, J.; Underwater measurements using laser induced breakdown spectroscopy. J. Anal. At. Spectrom., 2016. 31; 328-336.

Arca, G.; Ciucci, A.; Palleschi, V.; Rastelli, S.; Tognoni, E.; Trace element analysis in water by the laser-induced breakdown spectroscopy technique, Appl. Spectrosc. 1997. 51; 1102–1105.

Arp, Z.; Cremers, D.; Harris, R. D.; Oschwald, D.; Parker, G.R. Jr.; Wayne, D.; Feasibility of generating a useful laser induced breakdown spectroscopy plasma on rocks at high pressure: preliminary study for a Venus mission, Spectrochim. Acta Part B 2004. 59; 987–999.

Baker, E.T.; Tennant, D.A.; Feely, R.A.; Lebon, G.T.; Walker, S.L.; Field and laboratory studies on the effect of particle size and composition of optical backscattering measurements in hydrothermal vent plumes, Deep-Sea Research I, 2001. 48; 593-604.

Barbini, R.; Colao, F.; Lazic, V.; Fantoni, R.; Palucci, A.; Angelone, M.; On board LIBS analysis of marine sediments collected during the XVI Italian campaign in Antarctica, Spectrochim. Acta Part B, 2002. 57; 1203-1218.

Brech, F.; Cross, L., Optical microemission simulated by a ruby maser, Appl. Spectrosc., 1962. 16; 58.

Bulajic, D.; Cristoforetti, G.; Corsi, M.; Hidalgo, M.; Legnaioli, S.; Palleschi, V.; Salvetti, A.; Tognoni, E.; Green, S.; Bates, D.; Steiger, A.; Fonseca, J.; Martins, J.; McKay, J.; Tozer, B.; Wells, D.; Wells, R.; Harith, M.A.; Diagnostics of high-temperature steel pipes in industrial environment by laser-induced breakdown spectroscopy technique: the LIBSGRAIN project, Spectrochim. Acta Part B 2002. 57; 1181-1192.

Butterfield, D.; Massoth, G., Geochemistry of north Cleft segment vent fluids: Temporal changes in chlorinity and their possible relation to recent volcanism, J. Geophys. Res. 1994. 99; 4951.

Buzukov, A.; Popov, Y.; Teslenko, V., Experimental study of explosin caused by focusing monopulse laser radiation in water, Jour. Appl. Mech. Tech. Phys. 1969. 10; 701-708.

Caceres, J.; Lopez, J.; Telle, H.; Urena, A., Quantitative analysis of trace metal ions in ice using laser-induced breakdown spectroscopy, Spectrochim. Acta Part A. 2001. 56; 831-838.

Casavola, A.; De Giacomo, A.; Dell'Aglio, M.; Taccogna, F.; Colonna, G.; De Pascale, O.; Longo,S.; Experimental investigation and modelling of double-pulse laser induced plasma spectroscopy under water, Spectrochim. Acta, 2005. 60; 975-985.

Clegg, S.; Wiens, R.; Misra, A.; Sharma, S.; Lambert, J.; Bender, S.; Mewell, R.; Nowak-Lovato, K.; Smrekar, S.; Dyar, M.; Maurice, S.; Planetary Geochemical investigations Using Raman and Laser-Induced Breakdown Spectroscopy, Appl. Spec., 2014. 68; 925-936.

Cremers, D., Radziemski,L.J.; Handbook of Laser-induced Breakdown Spectroscopy. Chichester, West Sussex, England: John Wiley & Sons, 2006. Print.

Cremers, D.A., L.J. Radziemski, T.R. Loree, Spectrochemical analysis of liquids using the laser spark, Appl. Spectrosc., 1984. 38; 721-729.

Cremmers, D.; Radziemski, L.; Loree, T., Spectrochemical Analysis of Liquids Using the Laser Spark, Appl. Spec. 1984. 38; 721-729.

Daly, K.; Byrne, R.; Dickson, A.; Gallager, S.; Perry, M.; Tivey, M.; Chemical and biological sensors for time-series research: current status and new directions, Mar. Technol. Soc. J., 2004. 38; 121–143.

De Giacomo, A.; Aglio, M.; Pascale, O., Single Pulse-Laser Induced Breakdown Spectroscopy in aqueous solution, Appl. Phys. A. 2004. 79; 1035-1038.

De Giacomo, A.; Dell'Aglio, M.; De Pascale, O.; Capitelli, M., From single pulse to double pulse ns-Laser Induced Breakdown Spectroscopy under water: Elemental analysis of aqueous solutions and submerged solid samples, Spectrochim. Acta Part B. 2007. 62; 721-738.

Dickey, T.; The role of new technology in advancing ocean biogeochemical studies, Oceanography 2001. 14; 108–120.

Elderfield, H.; Schultz, A., Mid-Ocean ridge hydrothermal fluxes and the chemical composition of the ocean, Annu. Rev. Earth Planet. Sci. 1996. 24; 191-200.

Essin, M.; Radziemski, L.; Sneddon, J.; Detection of Cadmium, Lead and Zinc in Aerosols by Laser-Induced breakdown Spectroscopy, J. Anal. At. Spectrom. 1988. 3; 985-988.

Fichet, P.; Mauchien, P.; Wagner, J.F.; Moulin, C.; Quantitative elemental determination in water and oil by laser induced breakdown spectroscopy, Anal. Chim. Acta 2001. 429; 269–278.

Fichet, P.; Menut, D.; Brennetot, R.; Vors, E.; Rivoallan, A., Analysis by laser-induced breakdown spectroscopy of complex solids, liquids, and powders with an echelle spectrometer, Appl. Optics. 2003. 42; 6029-6035.

Fichet, P.; Toussiant, A.; Wagner, J., Laser-induced breakdown spectroscopy: A tool for analysis of different types of liquids, Appl. Phys. A. 1999. 69; S591-S592.

Gaudiuso, R.; Dell'Aglio, M.; De Pascale, O.; Senesi, G.S.; De Giacomo. A.; Laser induced breakdown spectroscopy for elemental analysis in environmental, cultural heritage and space applications: A review of methods and results, Sensors, 2010. 10; 7434-7468.

German, C.R.; Von Damm, K.L.; Hydrothermal processes Treatise on Geochemistry, H. Elderfield, H. D. Holland, and K. K. Turekian, eds. Elsevier. 2003. 6; 181-222.

Ingle, J.D.; Crouch, S.R. Spectrochemical Analysis. Englewood Cliffs, NJ: Prentice Hall, 1988.

Kumar, A.; Yueh, F.; Miller, T.; Singh, S., Detection of trace elements in liquids by laser-induced breakdown spectroscopy with a Meinhard nebulizer, Appl. Optics., 2003. 42; 6040-6046.

Kuvalchuk-Kogan, T.; Butatov, V.; Schechter, I.; Optical Breakdown in Liquid Suspensions and its Analytical Applications, Adv. Chem., 2015. 2015; 1-21.

Lawrence-Snyder, M.; Scaffidi, J.; Angel, S. M.; Michel, A.P.M.; Chave, A.D.; Laser-Induced Breakdown Spectroscopy of High-Pressure Bulk Aqueous Solutions, Appl. Spectrosc. 2006. 60; 786-790.

Lawrence-Snyder, M.; Scaffidi, J.; Angel, S.M.; Michel, A.;Chave, A. Sequential-Pulse Laser –Induced Breakdown Spectroscopy of High-Pressure Bulk Aqueous Solutions, Appl. Spec., 2007. 61; 171-176.

Lazic, V.; Jovicevic, S.; Fantoni, R.; Calao, F.; Efficient plasma and bubble generation underwater by an optimized laser excitation and its application for liquid analyses by laser-induced breakdown spectroscopy, Spectrochimica Acta Part B, 2007. 62; 1433-1442.

Lee W.; Wu J.; Lee Y.; Sneddon J.; Recent applications of laser-induced breakdown spectrometry: a review of material approaches, Appl. Spectrosc. Rev., 2004. 39; 27–97.

Luther, G.; Rozan, T.; Taillefert, M.; Nuzzio, D.: Meo, C.; Shank, T.; Lutz, R.; Cary, S., Chemical speciation drives hydrothermal vent ecology, Nature. 2001. 410; 813-816.

Majidi V.; Joseph, M.; Spectroscopic applications of laser induced plasmas, Crit. Rev. Anal. Chem. 1992. 23; 143–162.

Michel, A.; Chave, A.; Double pulse laser-induced breakdown spectroscopy of bulk aqueous solutions at oceanic pressures: interrelationship of gate delay, pulse energies, interpulse delay, and pressure, Appl. Optics. 2008. 47; G131-G143.

Michel, A.; Lawrence-Snyder, M.; Angel, S.M.; Chave, A., Laser-induced breakdown spectroscopy of bulk aqueous solutions at oceanic pressures: evaluation of key measurement parameters, Appl. Optics. 2007. 46; 2507-2515.

Miziolek, A.W.; Palleschi, V.; Schechter I.; Laser-induced Breakdown Spectroscopy (LIBS): Fundamentals and Applications. Cambridge, UK: Cambridge UP, 2006.

Mohamed, W.T.Y.; Quantitative elemental analysis of seawater by laser induced breakdown spectroscopy, Int, J. Pure Appl. Phys. 2006. 2; 11-21.

Moroz, V.I.; Studies of the atmosphere of Venus by means of spacecraft: Solved and unsolved problems, Adv. Space Res., 2002. 29; 215-225.

Munson, C.A.; De Lucia F.C. Jr.; Piehler, T.; McNesby, K.L.; Miziolek, A.W.; Investigation of statistics strategies for improving the discriminating power of laser-induced breakdown spectroscopy for chemical and biological warfare agent simulates, Spectrochim. Acta Part B, 2005. 60; 1217-1224.

Noda, M.; Deguchi, Y.; Iwasaki, S.; Yoshikawa, N.; Detection of carbon content in a high-temperature and high- pressure environment using laser-induced breakdown spectroscopy, Spectrochim. Acta Part B 2002. 57; 701-709.

Omenetto, N.; Hahn, D.; Laser-Induced Breakdown Spectroscopy (LIBS), Part I: Review of Basic Diagnostics and Plasma-Particle Interactions: Still-Challenging Issues Within the Analytical Plasma Community, Appl. Spec., 2010. 64; 335A-366A.

Paksy, L.; Német, B.; Lengyel, A.; Kozma, L.; Czekkel, J.; Production control of metal alloys by laser spectroscopy of the molten metals. Part 1. Preliminary investigations, Spectrochim. Acta Part B, 1996. 51; 279-290.

Pichahchy, A.; Cremers, D.; Ferris, M.; Elemental analysis of metals under water using laser-induced breakdown spectroscopy, Spectrochim. Acta Part B, 1997. 52; 25–39.

Radziemski, L.; Cremers, D.A.; Benelli, K.; Khoo, C.; Harris, R.D.; Use of the vacuum ultraviolet spectral region for laser-induced breakdown spectroscopy-based Martian geology and exploration, Spectrochim. Acta Part B 2005. 60; 237-248.

Radziemski, L.; Review of analytical applications of laser plasmas and laser ablation, 1987–1994, Microchem. J. 1994. 50; 218–234.

Rusak, D.; Castle, B.; Smith, B.; Winefordner, J.; Fundamentals and applications of laser-induced breakdown spectroscopy, Crit. Rev. Anal. Chem., 1997. 27; 257–290.

Rusak, D.; Castle, B.; Smith, B.; Winefordner, J.; Recent trends and the future of laser-induced plasma spectroscopy, Trend. Analyt. Chem. 1998. 17; 453–461.

Sallé, B.; Cremers, D.A.; Maurice, S.; Wiens, R.C.; Laser-induced breakdown spectroscopy for space exploration applications: Influence of the ambient pressure on the calibration curves prepared from soil and clay samples, Spectrochim. Acta Part B 2005. 60: 479-490.

Salle, B.; Lacour, J.L.; Vors, E.; Fichet, P.; Maurice, S.; Cremers, D. A.; Wiens R. C., Laser-induced breakdown spectroscopy for Mars surface analysis: capabilities at stand-off distances and detection of chlorine and sulfur elements, Spectrochim. Acta Part B, 2004. 59: 1413–1422.

Samek, O.; Beddows, D.; Kaiser, J.; Kukhlevsky, S.; Liska, M.; Telle, H. H.; Young, J.; Application of laser-induced breakdown spectroscopy to in situ analysis of liquid samples, Opt. Eng. 2002. 39; 2248-2262.

Scaffidi, J.; Angel, M.S.; Cremers, D., Emission Enhancement Mechanisms in Duel-Pulse LIBS, Anal. Chem. 2006. 41; 25-32.

Seyfried, W. Jr.; Johnson, K.; Tivey, M. C.; In-situ sensors: their development and application for the study of chemical, physical and biological systems at mid-ocean ridges, NSF_Ridge Sponsored Workshop Report (2000).

Seyfried, W.E., Jr.; Janecky D.R.; Mottl, M.J.; Alteration of the oceanic crust: Implications for geochemical cycles of lithium and boron, Geochimica Acta, 1984. 48; 557-569.

Sharma, S.; Misra, A.; Clegg, S.; Barefield, J.; Weins, R.; Acosta, T.;Time-resolved remote Raman study of minerals under supercritical CO2 and high temperatures relevant to Venus exploration, Phil. Trans. R. Soc. A, 2010. 368; 3167-3191.

Sharma, S.; Misra, A.; Singh, U.; Remote Raman Spectroscopy of Minerals at Elevated Temperature Relevant to Venus Exploration, SPIE 7153, Lidar Remote Sensing for Environmental Monitoring IX, 8 December 2008; doi: 10.1117/12.806371.

Sneddon, J.; Lee, Y.; Novel and recent applications of elemental determination by laser-induced breakdown spectroscopy, Anal. Lett. 1999. 32; 2143–2162.

Song, K.; Lee, Y.; Sneddon, J.; Applications of laser-induced breakdown spectrometry, Appl. Spectrosc. Rev. 1997. 32; 183–235.

Takahashi, T.; Thornton, B.; Sato, T.; Ohki, K.; Sakka, T.; Quantitative chemical analysis of submerged solids using calibration-free laser-induced breakdown spectroscopy. Proc. MTS/IEEE Oceans '14, St. John's, NL, 2014. 140326-120.

The next generation of in situ biological and chemical sensors in the ocean: a workshop report, (2004).
URL:http://www.whoi.edu/institutes/OLI/activities/symposia_sensors.htm.

Tivey, M.; Generation of Seafloor Hydrothermal Vent Fluids and Assocated Mineral Deposits, Oceanography. 2007. 20; 50-63.

Tognoni, E.; Palleschi, V.; Corsi, M.; Cristoforetti, G., Quantitative micro-analysis by laser-induced breakdown spectroscopy: a review of the experimental approaches, Spectrochim. Acta Part A. 2002. 57; 1115-1130.

Tran, M.; Sun, Q.; Smith, B.; Winefordner, J.D.; Direct determination of trace elements in terephthalic acid by laser induced breakdown spectroscopy, Anal. Chim. Acta, 2000. 419; 153-158.

Varney, M.; ed., Chemical Sensors in Oceanography (Gordon and Breach, 2000).

Von Damm, K.; Edmond, J.; Grant, B.; Measures, C., Chemistry of submarine hydrothermal solutions at 21˚N, East Pacific Rise, Geochem. Et. Cosmochem. Acta. 1985. 49; 2197-2220.

Von Damm, K.L.; Lilley, M.D.; Shanks W.C. III; Brockington, M.; Bray, A.M.; O'Grady, K.M.; Olson, E.; Graham, A.; Proskurowski G.; SouEPR Science Party, Extraordinary phase separation and segregation in vent fluids from the southern East Pacific Rise, E. Pl. Sci. Lett., 2003. 206; 365-378.

Wainner, R.T.; Harmon, R.S.; Miziolek, A.W.; McNesby, K.L.; French, P.D.; Analysis of environmental lead contamination: comparison of LIBS field and laboratory instruments, Spectrochim. Acta Part B, 2001. 56; 777-793.

Walker, S.L.; Baker, E.T.; Particle-Size Distributions within Hydrothermal Plums Over the Juan de Fuca Ridge, Mar. Geol. 1988. 78; 217-226.

Yui, H.; Kanoh, K.; Fujiwara, H.; Sawada, T.; Stimulated Raman scattering of liquid water under the strong focusing condition: analysis of local hydration network environments in dilute ethanol solutions, J. Phys. Chem. 2002. 106; 12041-12044.